Study of Biological Structure at the Molecular Level with Stereomodel Projections I. The Lipids in the Myelin Sheath of Nerve

F. A. VANDENHEUVEL, Animal Research Institute, Canada Dept. of Agriculture, Ottawa, Ontario

Abstract

Considerable uncertainty still exists regarding the detailed arrangement in protein-lipid molecular associations found in serum lipoproteins, plasma-membranes of cell organelles, the myelin sheath of nerve, and many other structures of paramount importance to biological mechanisms both in health and disease. Working hypotheses concerning such structures must eventually be tested by comparing known properties with those suggested by exact stereomodels. In this type of study, orthogonal projections of the molecules offer several advantages over the tri-dimensional stereomodels from which they can be derived by a described photographic process. The rules governing the configuration to be given the molecular models used for this purpose are discussed, and the possible applications of the resulting diagrams are described and illustrated by numerous examples taken in the lipid field.

These rules are then applied to the lipids in the myelin sheath of nerve. Striking similarities in the configurational features of the two main classes of myelin lipids, the phosphatidyl (dal) and the sphingolipids, immediately suggest very similar models for them.

On the other hand, numerous independent observations have indicated the highly probable occurrence of bimolecular complexes involving members of either class with cholesterol. Such complexes are exemplified by proposed models of cholesterol-lecithin and cholesterol-sphingomyelin units. It is demonstrated that the cohesional forces at play should indeed promote stable complexes of this kind.

All configurational features of the lipids in myelin fit these basic models. Dimensional variations induced by a broad spectrum of component fatty acids, affect only the length of the resulting complex units. Moreover, the tail-to-tail arrangement of these units provides paired elements of the same length. The latter corresponds exactly to the fundamental dimension predicted for the bimolecular leaflet by low angle X-ray diffraction studies on fresh, unfixed myelin.

A model of the bimolecular lipid leaflet produced by parallel grouping of the paired elements is discussed.

Introduction

THE SAFE control of biological function in health and disease will probably require detailed information on the configuration and organization of molecules in cellular structures attending to these functions. At this level it has not been possible so far to make observations or measurements that could be interpreted directly. To quote Fernández-Morán—"Recent methodological advances in high-resolution electron microscopy of biological specimens have made it possible to visualize directly structural detail of the order of 6–8 Å under favorable conditions, thus providing potential access to the molecular domain, where structure and function are indissolubly blended. Even if we succeeded hypothetically in attaining ideal preservation and resolution of the unit layers, however, the corresponding ultrastructural patterns would still remain figuratively classed as 'hieroglyphics,' waiting to be deciphered through detailed correlation with specific biochemical and biophysical data" (1).

Research on the molecular organization of biological structure must therefore follow the type of approach which consists in studying a 3-dimensional model embodying structural features suggested by the data available. The ability of this tentative model in explaining properties of the structure under investigation is then checked, often through new, carefully designed experiments. Through a sequence of conceptual amendments induced by the resulting observations, a model should be obtained from which reasonably accurate predictions may be made concerning structural behaviour under a wide range of conditions.

It should be obvious that the usefulness of these models can be severely curtailed by errors in atomic parameters and configuration principles used in their construction. The type of model is important also since those presenting an open structure are inherently better suited to work of this kind. Among other advantages, they do not conceal the framework of atom-to-atom bonds which often suggests interesting relationships.

In this type of research, an accurate and useful record of models at various stages of development can best be obtained through the graphical representations known as *orthogonal projections*. It is the purpose of this paper to show how accurate representations of this type can be conveniently obtained from open atomic stereomodels of the Dreiding type (Swissco Instruments, Greenville, Ill.). In addition, it will be shown how such projections can be used instead of the models themselves in the search for structural organization.

Orthogonal Projections have been known and used for a long time under the more familiar names of plane, elevation, end view, side view, top view, etc. . . by mechanical designers and architects. The principle involved is illustrated in Figure 1a. Here a tetrahedron is placed near three planes of reference (H,V,V′) perpendicular to each other, and the projections of this object are obtained by drawing through apices A,B,C,D, lines at right angle (thus orthogonal) to those planes. Although only two such projections are necessary to give a complete and accurate graphical description of a 3-dimensional object, projections in other planes, usually in one perpendicular to the first two, are often desirable. Usually, the object is placed with its principal long axis par-

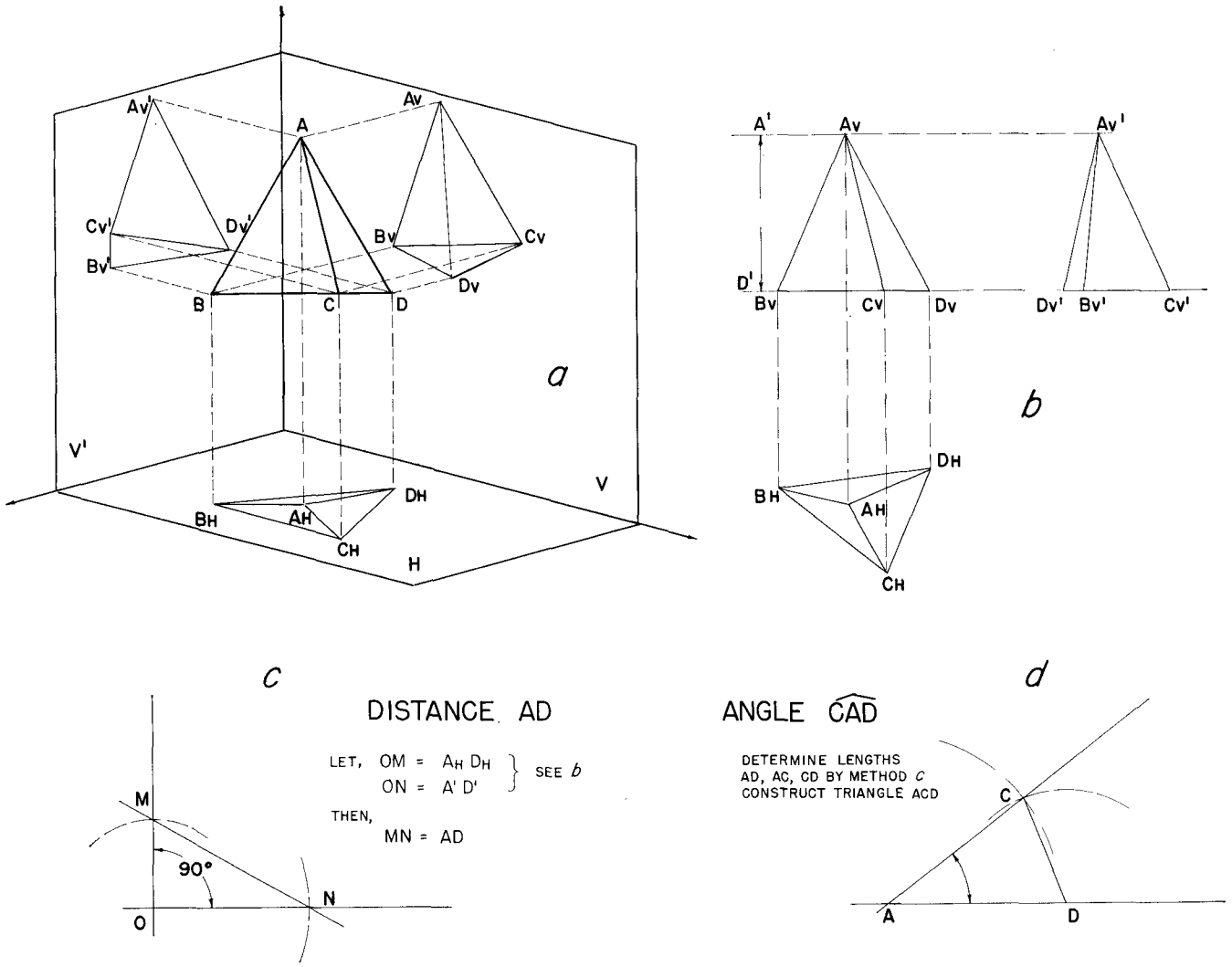

FIG. 1. a) Orthogonal projections of tetrahedron ABCD; in horizontal plan H, AA_H,BB_H,CC_H,DD_H are $\perp$ H; in vertical plan V,AA_V,BB_V,CC_V,DD_V, are $\perp$ V, etc... ; b) conventional representation of projections; c) measuring actual distance AD from projections; A'D' (Fig. 1b) is elevation A above D; d) measuring angle CAD; angle can also be calculated from values of AC,CD, and AD by trigonometry.

allel to the two first planes and the projections commonly designated as top view, side view, and end view are conventionally arranged as shown in b. A set of this type permits the measurement of any distance between structurally important points and of any angle between two structural lines by the simple processes described in c and d. Furthermore, it permits the construction of projections representing the object in any position in relation to the initial reference planes, and therefore, in any position in relation to other objects. Consequently, orthogonal projections of simple molecular models can be used to represent complex molecular associations no matter what relative position the various elements occupy. This result can be accurately achieved through the application of simple drafting procedures familiar to design engineers and draftsmen. These are fully described in specialized manuals, for example, in reference (2).

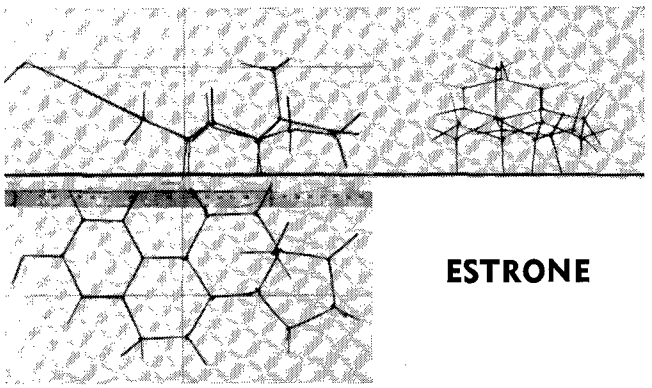

FIG. 2. Positive copies from photographs of a Dreiding model of the estrone molecule showing arrangement of photographs in view of constructing the final diagram shown in Figure 3.

In open molecular models of the Dreiding type the structural points of importance are the centers of all atoms. To obtain a set of orthogonal projections from such models by direct mensuration and drafting constitutes a very tedious operation. In an article to appear shortly in J.Photog.Sc. (3), a method is described for obtaining accurate projections by distant photography of Dreiding models. The process is based on the fact that orthogonal projections may be regarded as views or photographs of the model from an infinite distance.

A photograph taken from a finite distance yields an image which, in relation to an orthogonal projection, is affected by parallax distortion. While the errors involved can be accurately corrected, they become negligible when the photograph is taken

from a sufficiently long distance. Thus scaled up enlargements corresponding to orthogonal projections can be obtained directly by the use of long focal optics. For relatively small models, *viz,* 30 cm, the distance and focal length required are 85 ft and 1000 mm, respectively. Inexpensive optics ($60) can be used for this purpose. For larger models, proportionally longer distances and focal lengths involving more expensive equipment (Questar, New Hope, Pa.) must be used. Enlargements at a convenient scale, 1 or 2 cm/Å, are finally obtained on non-shrinkable film (Fig. 2) and final diagrams (Fig. 3), of which several examples are given below, are obtained by transferring to non-shrinkable, plastic tracing material, the position of all atom centers, joining these centers in the appropriate sequence and drawing the respective van der Waals radii of atoms.

Configuration. All techniques so far described involve relatively simple routine procedures. To produce a model having a configuration which, among many possible ones, will give the best expression of the data, involves interpretation of the forces underlying the molecular associations present in biological structures. The physical forces at play in this particular area are not conducive to the formation of perfectly stable compounds. Rather they promote the formation of molecular complexes in which the positions and configuration of individual molecules are affected by thermal agitation. However, the combined effect of these forces is large enough to induce most of the molecules to stay most of the time in positions and configurations that will ensure the durability of the structure as a whole. Equilibrium configurations and positions corresponding to the highest statistical probability must therefore exist. Since these should also correspond to the largest resultant of all cohesional forces, a quantitative estimation of the latter constitutes a reliable guide in estimating the most probable molecular arrangements. In this connection, it is useful to consider that the energy requirements per mole for the formation of a stable complex is from 10–15 times kT, i.e., 10–15 times the energy associated with thermal motion or from −6 to −9 Kcal. at room temperature (4,5).

TABLE I

van der Waals Radii of Atoms [a]

		H	1.2 Å		
N	1.5 Å	O	1.40 Å	F	1.35 Å
P	1.9 Å	S	1.85 Å	Cl	1.80 Å
As	2.0 Å	Se	2.00 Å	Br	1.95 Å
Sb	2.2 Å	Te	2.20 Å	I	2.15 Å

[a] From Pauling (7). © 1960, Cornell University, by permission of Cornell University Press.

Forces—The forces at play result from London-van der Waals, hydrogen bond, ionic bond, and dipole-dipole interactions.

London-van der Waals effects are manifested by concomitant repulsive and attractive forces arising between nonbonded atoms. Such forces become appreciable when internuclear distances decrease below about 6 Å, and increase exponentially as the atoms approach the equilibrium position which they assume in crystals. This position corresponds to a distance from center to center which equals the sum of the van der Waals radii, and is characterized by a maximally attractive net force. As electron fields further interpenetrate, the positive component increases more rapidly and the resultant force becomes

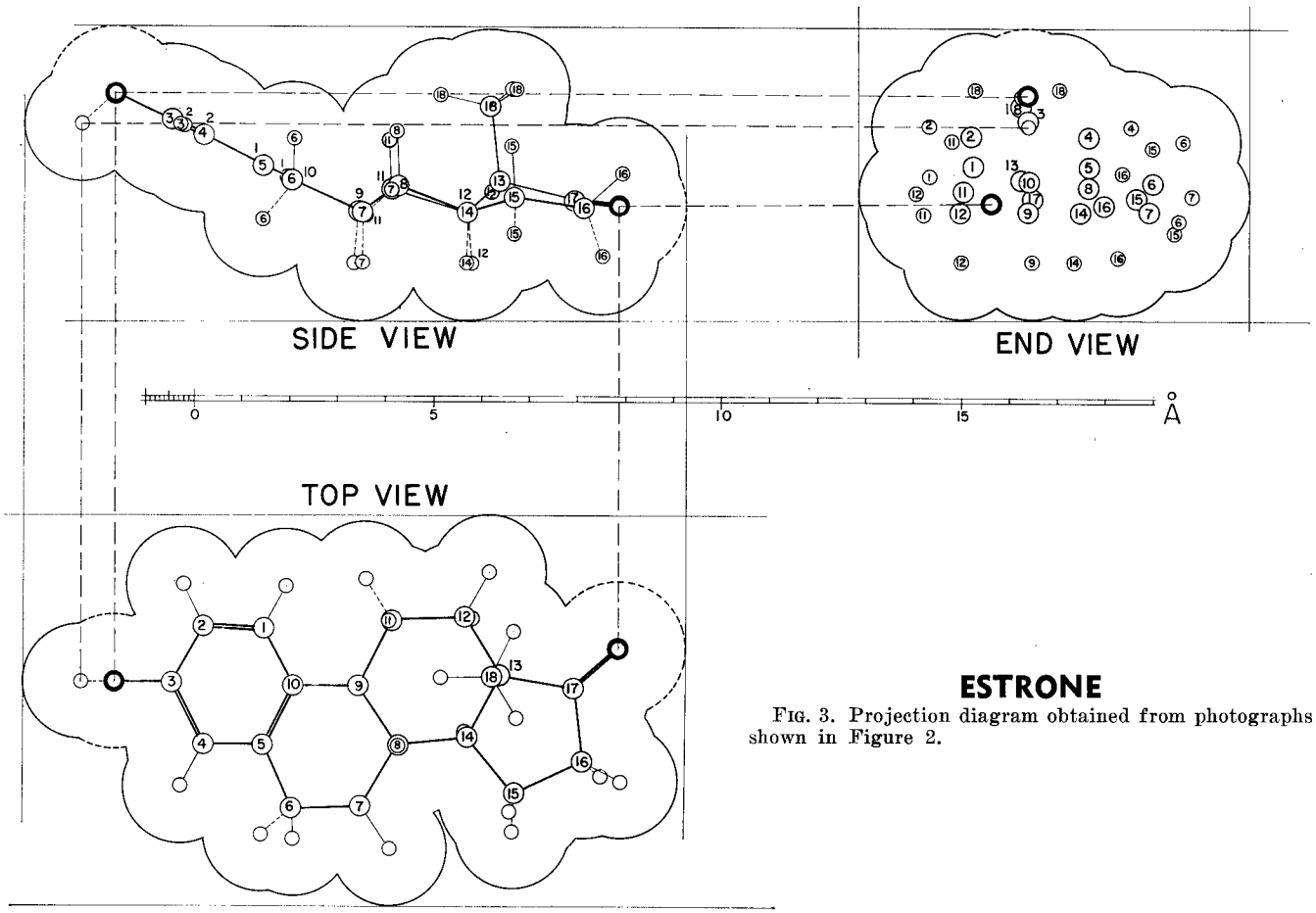

FIG. 3. Projection diagram obtained from photographs shown in Figure 2.

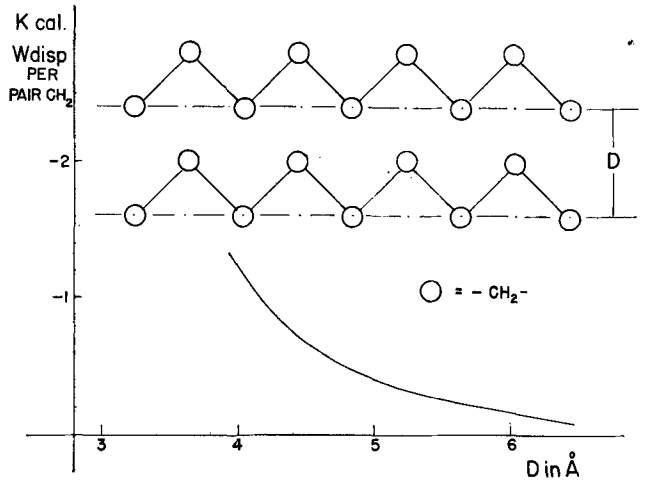

FIG. 4. Curve obtained by plotting against D (distance in Å between planes containing C atoms in parallel chains), the van der Waals interaction for one pair of $-CH_2-$. This was calculated using Salem's expression [8],

$$W_{disp} = A \frac{3\pi}{8l} \frac{N}{D^5}$$

where W_{disp} is the total interaction, A = −1340 Kcal./mole, *l*, the effective C–C distance along the chain (1.253 Å), and N, the number of CH_2 pairs. This expression is valid for $D \geqslant 4$ Å (11).

strongly repulsive. This behaviour is described by the following general expression for the resultant force V,

$$V = A\, r^{-12} - B\, r^{-6}$$

known as the Lennard-Jones "6–12" potential. In this expression, A and B are positive constants for the repulsive and attractive component respectively, and r, the distance between centers. Many expressions for specific atoms and specific ranges have been proposed (6).

A list of van der Waals radii reproduced from Pauling (7) is given in Table I.

The van der Waals radius of hydrogen is 1.2 Å, and it follows from the above definitions that the closest approach for two hydrogen atoms located on different molecules is 2.4 Å from center to center. The same rule applies to hydrogen atoms on the same molecule when they belong to nonbonded carbon atoms. Exceptions to this rule are found when the carbon atoms are in the 1–3 position and when one or both these atoms are located in a rigid carbon-carbon skeleton, for instance, the body of the cholesterol molecule. Hydrogen atoms attached to carbons in these situations may have to come closer than 2.4 Å, or even 2 Å as models clearly show. It would seem logical that in these and other cases when two or more atoms cannot be positioned at normal equilibrium distances, the most probable configuration should be that which corresponds to a balance of repulsive forces for all atoms concerned.

Repulsive forces between atoms attached to bonded atoms are an important consideration in regard to the configuration of fatty acid chains. There is convincing evidence for potential barriers restricting free rotation about C–C bonds (8). Although the energies involved cannot be accurately predicted (9), they have been measured in many cases. Thus the value corresponding to rotation of $-CH_3$ groups around the C–C bond of ethane is 3 Kcal., while in other cases values up to 7 Kcal. have been recorded (10). While molecules in the liquid state may afford free rotation within restricted angles, those in ordered, restrained association such as are being considered

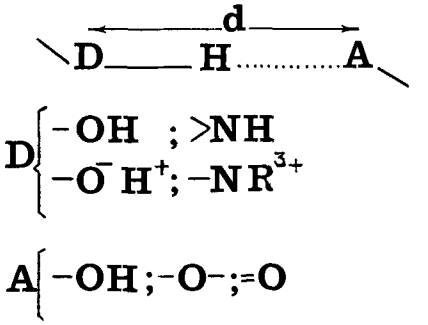

FIG. 5. Functional groups in lipid complexes, capable of forming hydrogen bonds. D is proton donor group, A is acceptor. Distance d varies between 2.5 and 3.4 Å.

presently, will be further restricted. In this respect the situation in the para-crystalline edifice of some membranes must be much closer to that found in the solid state. Thus the statistically most probable configuration of flexible, chain-like appendages in this situation should be the planar staggered one corresponding to maximum distance between nonbonded atoms. Such configuration is characterized by the absence of repulsive interaction, i.e., by the lowest possible level of energy.

Given a model, van der Waals interactions can be estimated fairly accurately. The computation is complicated by the fact that interactions of each atom with every other atom must be calculated separately and the results then compounded. However, for models such as two fatty acid chains, Salem has given a simple expression of these forces (11). A graph representing this expression is shown in Figure 4. For two straight 18 carbon chains in closest contact, D = 4.17 Å and the attractive energy W is −18.0 Kcal., a considerable amount.

Hydrogen Bond Interactions which are of interest in a study of lipid-lipid complexes, involve oxygen and nitrogen atoms only, according to the simple scheme shown in Figure 5. Here the proton donor atom D, the hydrogen atom covalently linked to it, and acceptor atom A must be colinear (12,13). Methods of estimating hydrogen bonding energies have been proposed (14,15). In general these energies lie between −2 and −8 Kcal.

From the variety in both donor and acceptor forms depicted in this figure, it would seem that the possible combinations involved in hydrogen bonding are numerous. However, because of the bulkiness of adjacent lipid molecules, and also because of their restricted mobility both within the complex and within the lipid monolayer, the distances between potential acceptor and donor groups will generally be too large, and the essential colinearity condition impossible to bring about. The chances for indirect hydrogen bonding through water molecules between potential donor or acceptor atoms of the lipid complex are much greater, particularly if the molecular species involved have an affinity for water. In this case, the bridging water molecules themselves will probably be connected to the network of water molecules bound to the superstructure of the lipid monolayer.

Distances, and the dielectric shielding effect from interposed water molecules of relatively low mobility would not seem favourable to direct *electrostatic (Coulombic) bonding* between adjacent lipid molecular complexes. Ionic interaction with limbs of the superficial protein, or with omnipresent inorganic

ions, would seem far more probable, and so would seem indirect bonding to the protein through multivalent cations (16). Inasmuch as changes in membrane superstructure should bring about changes in membrane properties, the latter will be induced by compositional variations in the adjacent aqueous phase, capable of shifting the equilibrium of competing forces (ionic, hydrogen bonding) between water and the various ionic species (lipid, inorganic, and protein). Hence a change in the concentration of inorganic ions or any competitive substance, should produce alterations of membrane properties that can only be explained by taking all forces and reactants into account. Plagued by oversimplification in this matter, the present studies of membrane properties offer a bewildering array of views and theories.

The very weak *dipole interactions* cannot play a significant role in lipid complex formation (11).

Practical Applications

A. *Single Molecules*—Application of some of the principles and techniques just discussed are illustrated by the following series of examples. Figure 6 shows projections of the progesterone molecule from a model where atoms which are not part of the rigid polycyclic frame were given positions such that possible interactions with neighbouring atoms would be balanced. After placing one of the three hydrogen atoms on C_{18} at equal distance from hydrogens in C_8 and C_{11}, the C_{20} carbonyl oxygen was placed at equal distance from the two remaining C_{18} hydrogens. The resulting configuration is that which Rakhit and Engel have recently proposed for this compound, as the more probable one in the light of much chemical and physical evidence (17). Extending this principle to the cholesterol molecule results in the tail configuration described in Figure 7.

Attempts to equilibrate possible interactions of hydrogen atoms linked to carbon 20,21 and 22 with neighbouring hydrogen atoms including those in C_{16}, C_{17},C_{18}, invariably lead to the configuration shown for C_{20} and C_{21}, and to the conclusion that this part of the tail is quite rigid. Consequently, only two possible positions would exist for carbons 22 and 23. The number of possible configurations for the end of the tail is restricted by the bulk of the methyl groups and is further restricted if the compact arrangement shown in Figure 7 is imposed. This type of configuration is of interest in relation to monolayers and membranes. Figure 8 shows the pattern obtained by arranging molecules of cholesterol in this configuration in such a way that they occupy the minimum possible space. The process through which this was obtained from the preceding orthogonal projections was described in a previous paper (18). The result indicates a cross sectional area of 37.9 Å^2 for the cholesterol molecule in excellent agreement with a value of 37.6 Å^2 for the limiting area of the cholesterol molecule obtained with the film balance (19). This is one among many examples (loc. cit.) indicating the reliability of orthogonal projections obtained by the process described. It also serves to point out that molecules in films having a high degree of cohesion fit closely together, even at very low surface pressure.

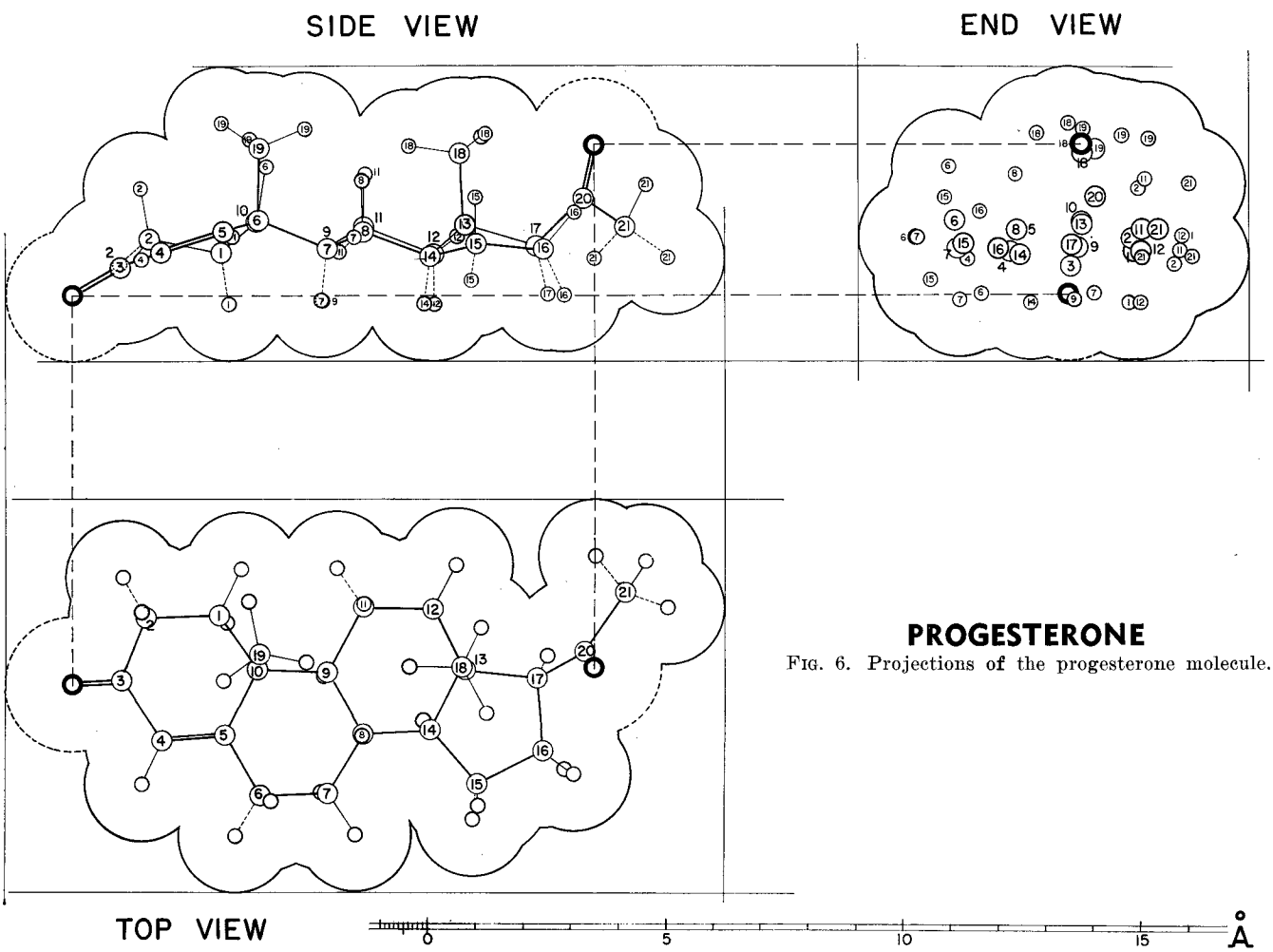

FIG. 6. Projections of the progesterone molecule.

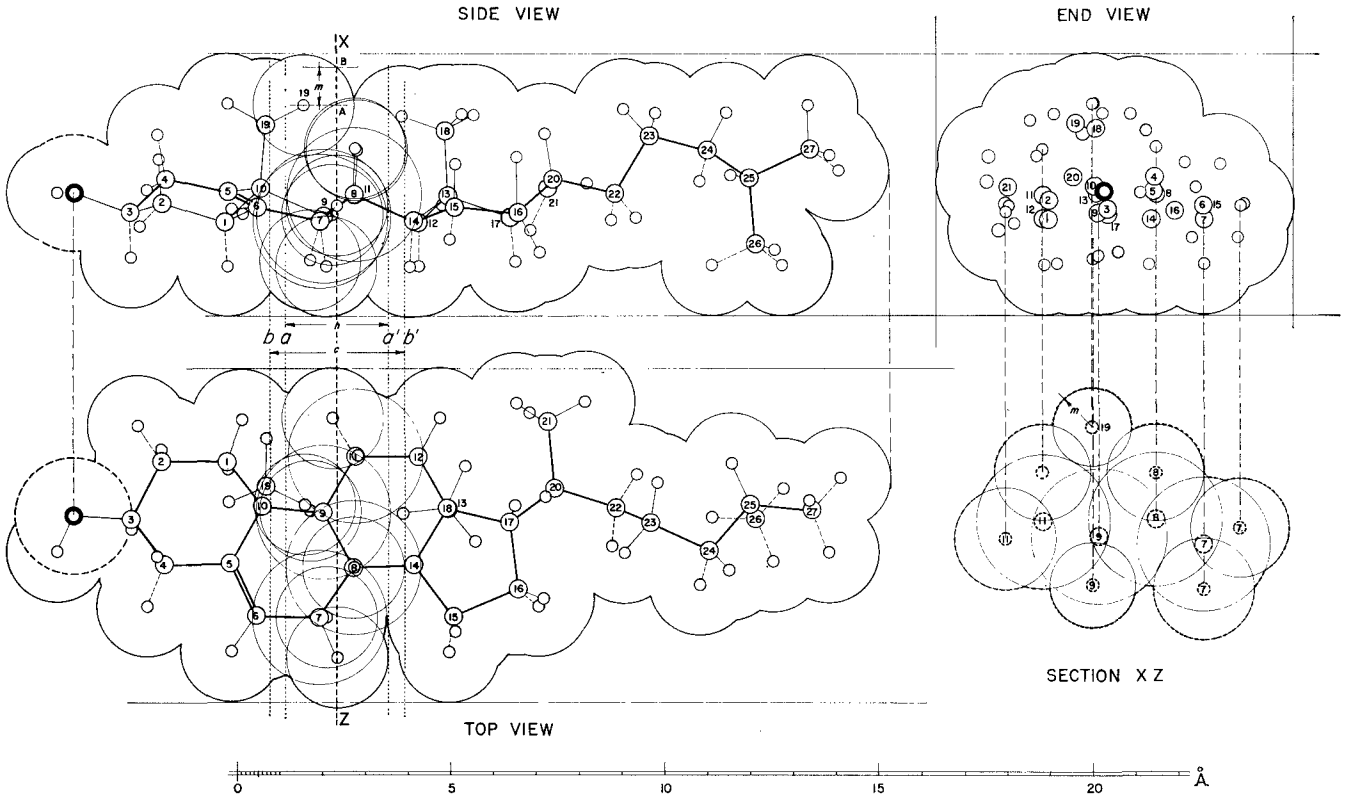

CHOLESTEROL

FIG. 7. Projections of the cholesterol molecule. Method for determining sections is described. In section by plan XZ, sections of all H atoms within aa′ = 2.4 Å, and of all C atoms within bb′ = 3.2 Å are included; h and c are van der Waals diam of H and C atoms, respectively. Method for determining radii m of sectioned atoms is exemplified for H on C_{19}. Positions of centers of atom in sections are taken from end view. One use of sections is described in Figure 8. See also (18). Note high density of atoms in region *closest* to face opposite C_{18} and C_{19}.

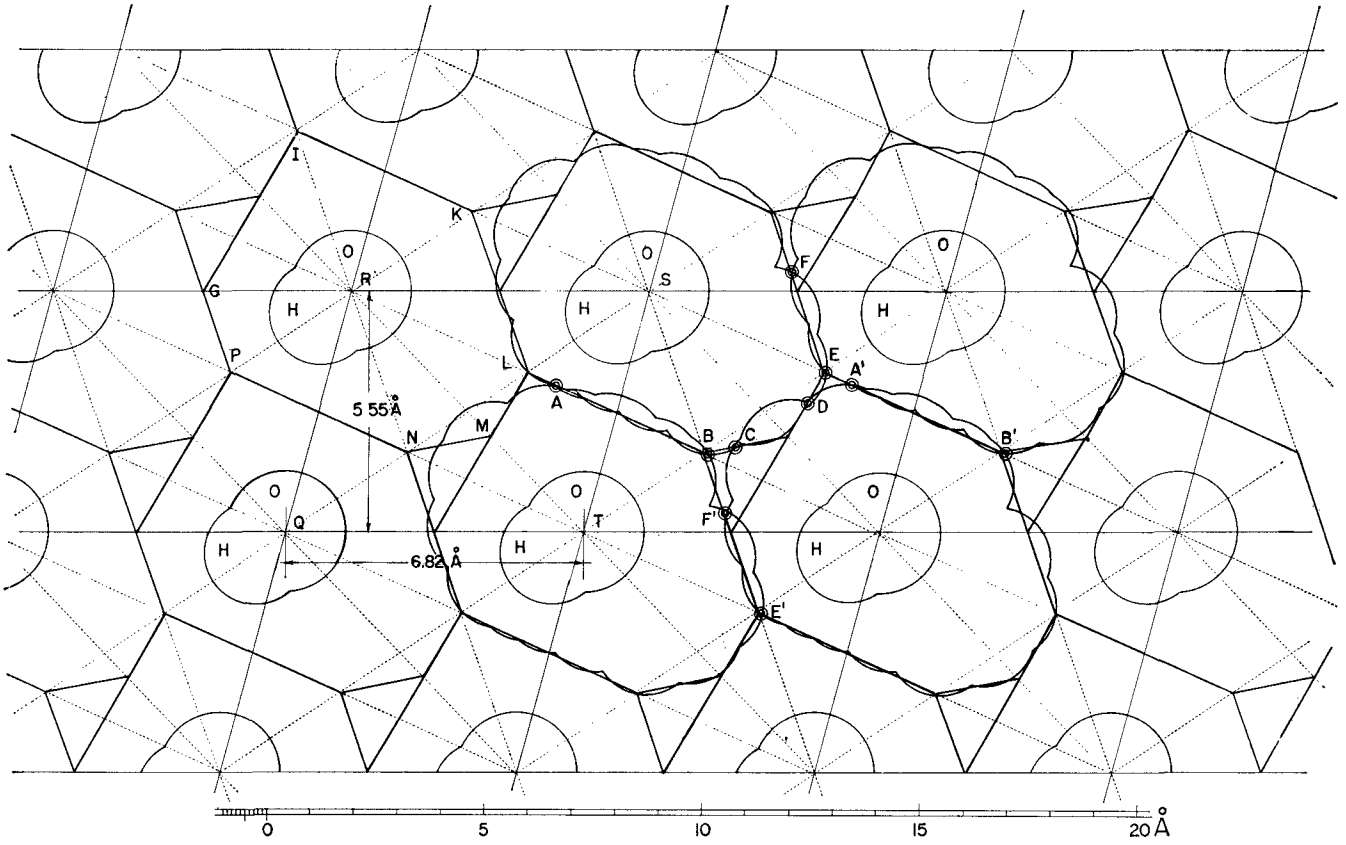

CHOLESTEROL MONOLAYER 37.9 Å²/MOL.

FIG. 8. Cholesterol monolayer arrangement. Molecules are ⊥ to, and —OH groups in contact with the water surface. This diagram is derived from end view and section data shown in Figure 7 by method described in previous paper (18). Improved method resulted in better agreement with observed area (37.6 Å²).

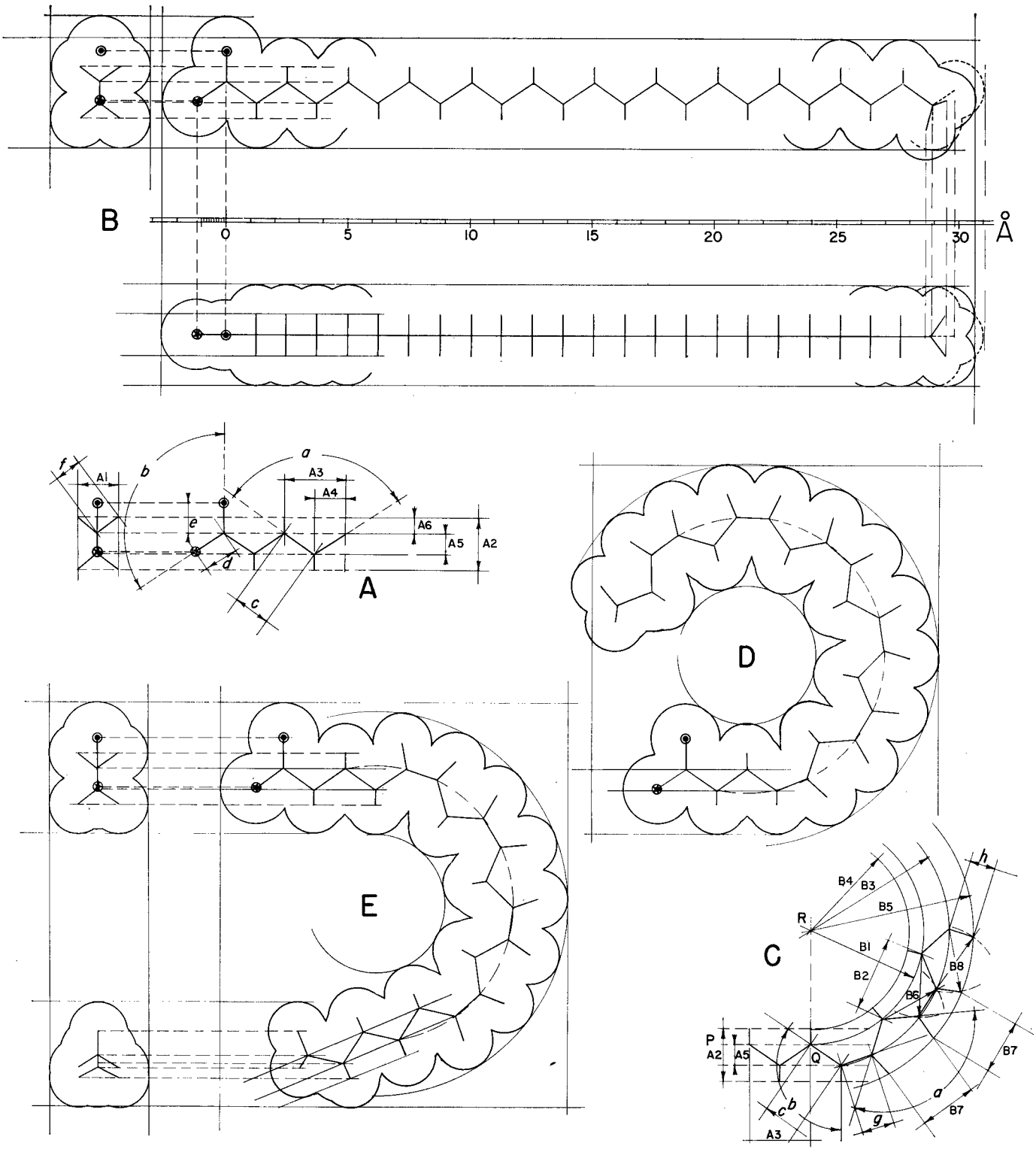

FIG. 9. (A) The parameters of straight chain acids. (B) Projections of lignoceric acid. (C) The parameters of the *cis*-double bond and method of construction for methylene-interrupted *cis*-double bond chains. (D) Methyl arachidonate (Me − $C_{20}\Delta 5,8,11,14$). (E) Methyl docosahexaneoate (Me − $C_{22}\Delta 4,7,10,13,16,19$).

Another example concerning single molecules is shown in Figure 9 which describes a study of fatty acid chains. The more recent and accurate values for paraffinic and ethylenic chain parameters were used and the configurations given these chains are those corresponding to a principle already discussed. Thus, in the case of the saturated acids described in B, and in the case of the unsaturated ones exemplified in E and D, all carbon atoms are coplanar and all methylene groups are staggered regularly in a *trans* position for neighbouring methylene groups or hydrogen atoms attached to double bonded C atoms. Minimum intramolecular interaction is thereby ensured. In this study, *cis* double bonds and

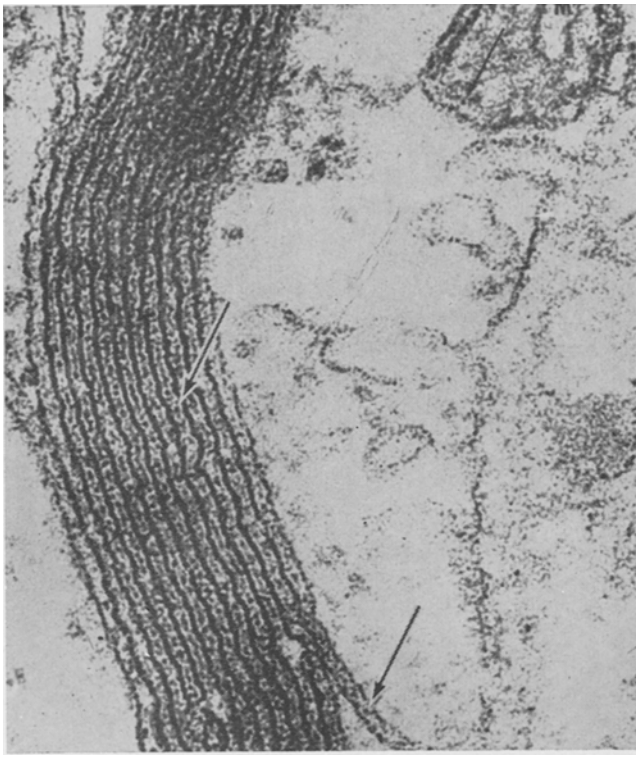

FIG. 10. Electron micrograph of osmium-fixed section of myelin sheath. Note jagged appearence of dense lines. From Fernández-Morán (1).

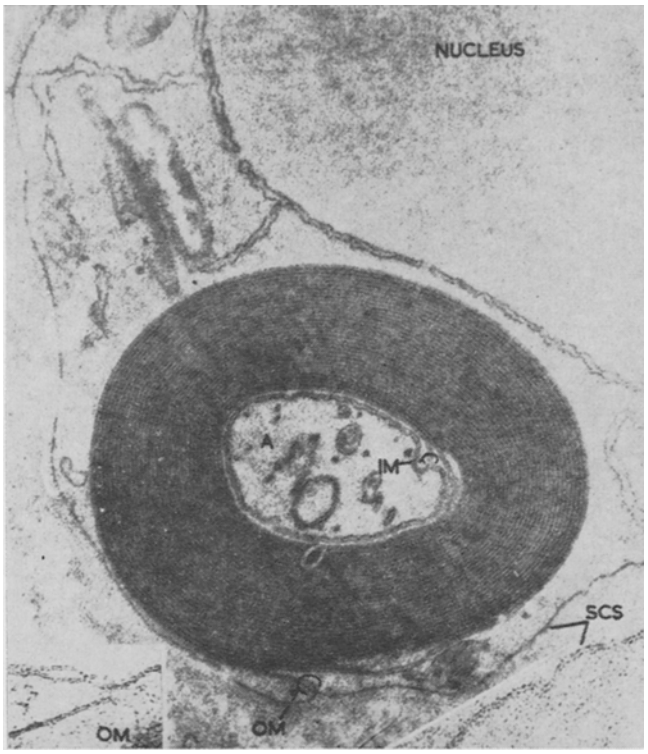

FIG. 12. Myelinized axon (A). IM, inner mesaxon; SCS, Schwann cell surface; OM, outer mesaxon. From Finean (33). By permission of the American Heart Association, Inc.

methylene interrupted series of *cis* double bonds only, have been considered. Calculations showed that all atoms in the methylene interrupted sequences lie on concentric circles, as shown. A simple method of construction, depicted in C was evolved on that basis. The parameters used in these constructions are given in Table II.

It must be pointed out that the theoretical 125°27′ was used for the C—C=C angle, in accordance with most observations (20), and that the Dreiding models, unfortunately, are inexact in this respect. Although this is easily corrected by using parameters given in Table II, it is often more expeditious and also more exact to draw unsaturated chains according to the procedure described.

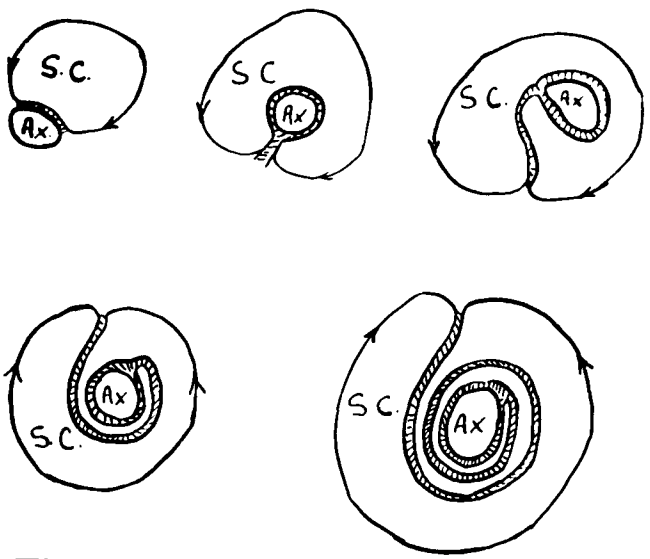

FIG. 11. The process of myelinization. Invagination of nerve axon (Ax) in Schwann cell (SC) followed by wrapping of successive layers of SC membrane around axon. From Geren (26).

Multimolecular System, Biological Structures

The example chosen for this demonstration is the myelin sheath of nerve (Fig. 10). It was only recently that the myelin of nerve (Fig. 11) was shown to result from the Schwann cell membrane wrapping itself around the nerve axon in concentric layers (26,27,28). However, it had long been known (29,30) that the latter presented characteristics of the paucimolecular membrane model proposed by Danielli

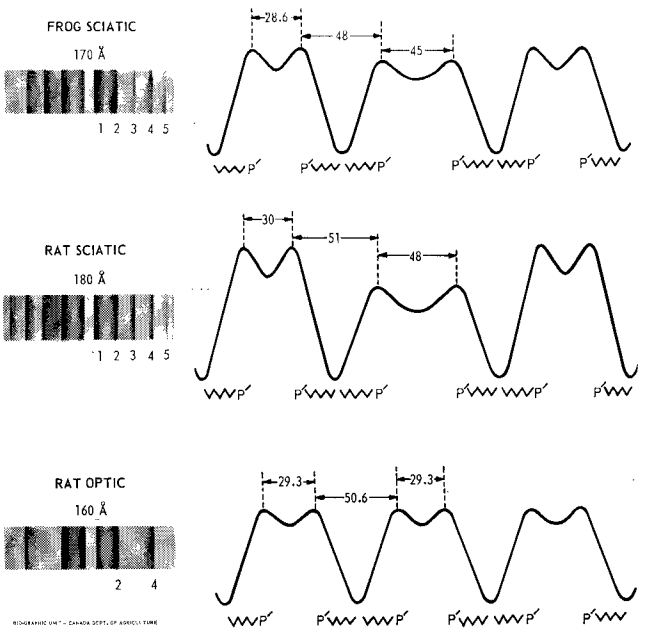

FIG. 13. Right: Low angle X-ray diffraction patterns of fresh, unfixed myelins; left, corresponding electron density curves. Methods described by Finean (33). By permission of the American Heart Association, Inc.

TABLE II
Known and Calculated Atomic Parameters of Fatty Acid Chains.
(see Fig 6)

Known Parameters	Ref.	Calculated		
a 109°28′	(21)	A1 1.788 Å	B1	4.63 Å
b 125°27′	(20)	A2 2.145 Å	B2	3.10 Å
c 1.535 Å	(8,22,23,24)	A3 2.506 Å	B3	5.65 Å
d 1.34 Å	(22)	A4 1.253 Å	B4	4.00 Å
e 1.24 Å	(25)	A5 0.883 Å	B5	6.65 Å
f 1.095 Å	(21)	A6 0.631 Å	B6	2.55 Å
g 1.335 Å	(8,22,23,24)		B7	2.30 Å
h 1.086 Å	(23)		B8	2.60 Å

and Davson (31). Finean showed that the myelin sheath (Fig. 12) itself accounted for about 80% of the total dry mass of peripheral nerve tissue (32). In a recent summary of the results of his very thorough electron microscope and X-ray diffraction studies (33) he showed the following figure (Fig. 13). On the left are seen the low-angle X-ray diffraction patterns of fresh, unfixed frog, and rat nerve myelin, and facing these patterns, the electron-density distributions derived from them. In these curves, peaks are assumed to arise from the phosphorus atoms (P′) in phospholipids arranged tail to tail. The reflections observed would therefore result from a symmetrical alignment of bimolecular lipid leaflets of constant width, the phosphorus atoms being about 51 Å apart. This does not, however, give any clue as to the molecular organization between and within the lipid leaflets.

In 1952, Finean proposed a model of the cholesterol-phospholipid complex (34) which has since

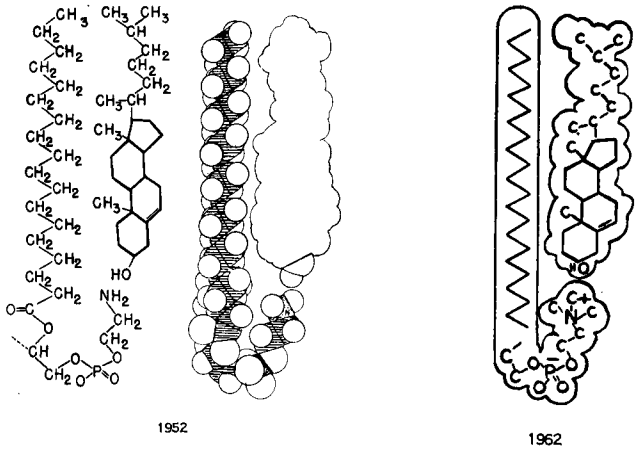

FIG. 14. Model of cholesterol-lecithin complex proposed by Finean (33,34).

been referred to without major modifications (Fig. 14). It explained the presence of large quantities of cholesterol in the myelin sheath, and introduced the concept of orderly and compact arrangement of lipids. The bend given to the phosphatidic chain, later described as the "walking stick" configuration, resulted from the belief that "the longest lipid molecules appear to be tilted or curled in some way so that they do not contribute their fully extended length to the thickness of the leaflet" (loc. cit.). Obviously, in 1952 as today, it was a problem to explain the observed thickness of the lipid layer. In this model,

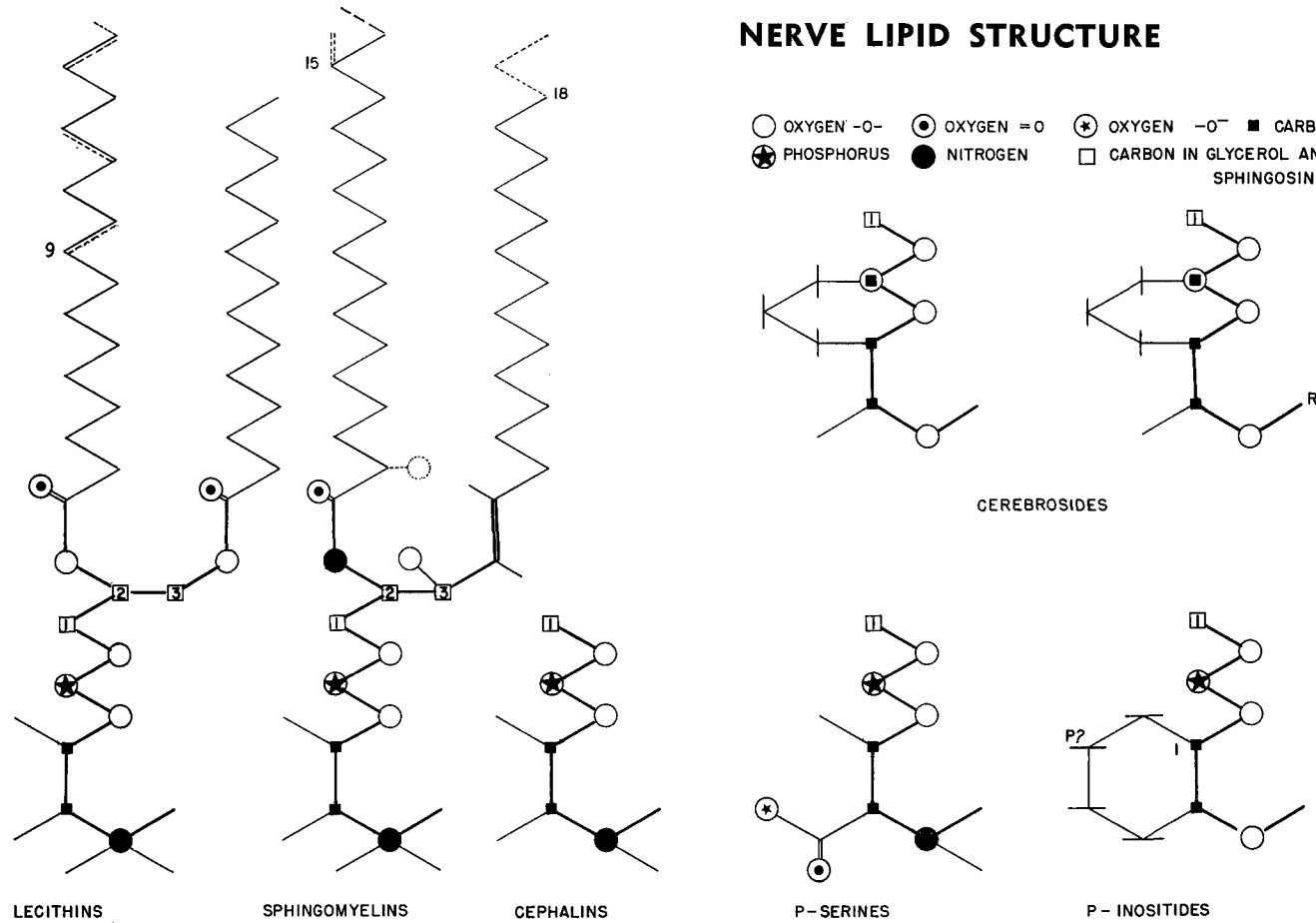

FIG. 15. Diagram showing similarity in structural features of phosphatidyl- and sphingolipids. Chain on C_2 in glycerol of lecithin generally unsaturated (43). The fatty acid chain linked to C_2 of sphingosine can be saturated or monounsaturated. The single double bond when present is in C_9 for 18- and 20-carbon chains, in C_{11} for 22- and C_{15} for 24-carbon chains. This chain can also bear —OH on α carbon. In phosphoinositides, position of phosphate on inositol probably C_5. In cerebrosides, R can be sulfuric or sialic acid.

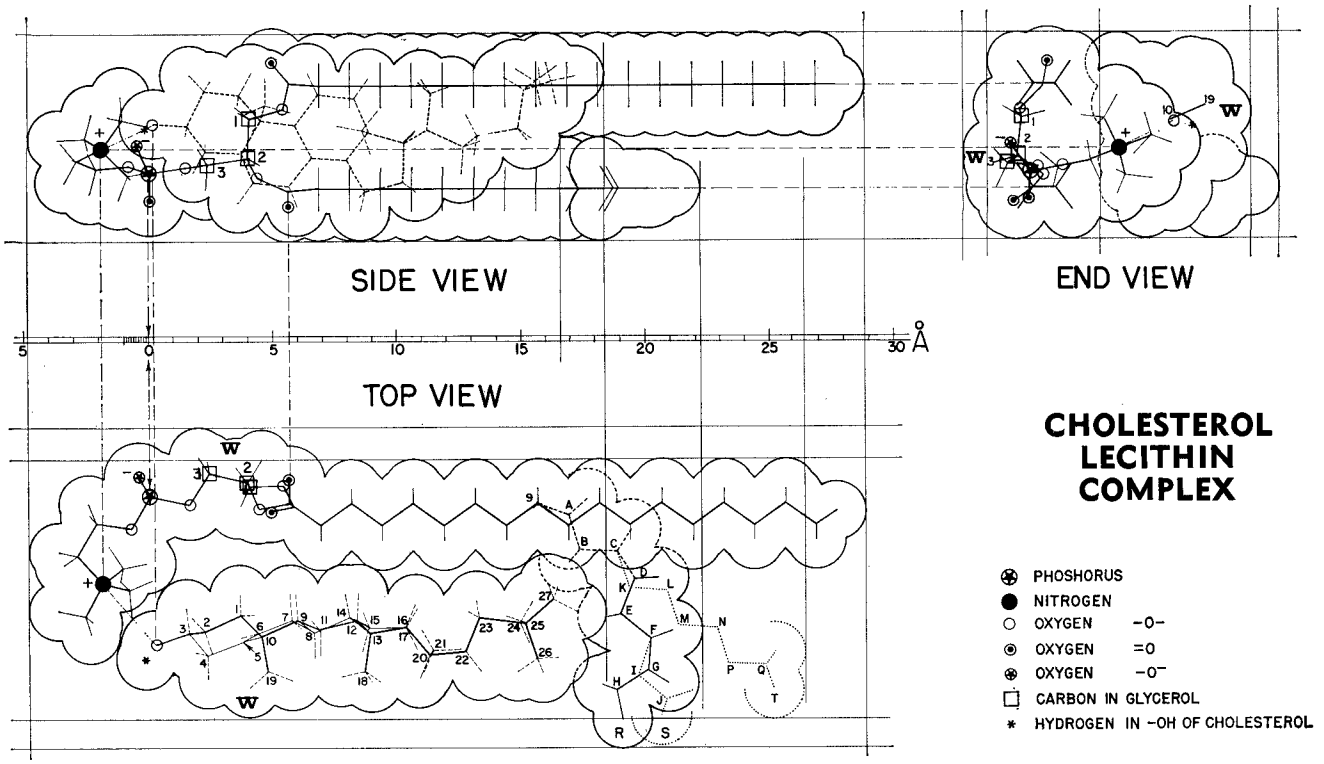

FIG. 16. Unsaturated chain on C_2 of glycerol in C_{18}-lecithin can be linolenic (9 — ABCDEFGH— R), linoleic (9 — ABCDEFIJ — S) or oleic (9 — ABCKLMNPQ — T). Obstacle to cholesterol: Hydrogens on C_{11},C_{13}, and C_{14} of fatty acid chain (atoms B,K, and E).

the position of the cholesterol molecule, within the complex, is obviously determined by this configuration. However, Finean found justifications for the bending of the phosphatidic chain by assuming a hydrogen bond between the —OH group of cholesterol and the terminal group of the phosphatidic chain. The likelihood of complex formation, explained on the basis of van der Waals interaction between the two molecules, was thereby enhanced.

Willmer recently (35) pointed out that this model did not fit observations by Dervichian (36) of a 55 $Å^2$ cross-sectional area per molecule in an equimolecular monolayer of cholesterol and lecithin. In addition, this configuration could not be reproduced with models of the lecithin molecule in this form. In fact, the model proposed by Finean is unsatisfactory on several other counts. First, it is still unable to explain the phosphorus- to phosphorus distance of about 50 Å without additional assumptions regarding the arrangement in opposition of a very large number of very long chains. These would have to be alternating, tilted, or bent-interlocking, for example. Second, it is incompatible with the occurrence of a considerable proportion of fatty acids with unsaturation starting at C_9 among the phosphatidyl components of myelin since the cholesterol molecule in this model undoubtedly stands in the way of such chains. Thirdly, a hydrogen bond such as suggested could not possibly arise between the —OH group of cholesterol and most terminal groups of the phosphatides and other lipids positioned as in this model, if only for lack of colinearity of the atoms involved. Finean himself suggested the possibility of an H— bond with the amino group of ethanolamine only. The ionic attractions assumed to occur in other cases could only be weak ion-dipole attractions. These could not contribute very much to complex stability or even justify the bending of phosphatidic chains. Much larger forces would be required to explain the bending of these chains which are strongly hydrophilic (19) and undoubtedly carry a tightly bound collar of water molecules that could oppose such configuration. Finally, the position of the cholesterol molecule in this model is not that which is conducive to the largest possible van der Waals interactions. This molecule (Fig. 7) features a large concentration of carbon atoms approximately located in a plane at only 2.5 Å from the outer face opposite the C_{18} and C_{19} methyl group. This is the face one would expect to be attracted most strongly by the lipid chains, since it would promote a total interaction about five times greater.

In spite of its shortcomings, Finean's model was important in bringing to the fore the concept of a cholesterol-phosphatide complex which, in one form or another, has since been used very widely. Evidence for the existence of such complexes accumulates. The more recent evidence is found, for example, in the results of Kramér (37) on the cholesterol-phospholipid ratio in serum β-lipoprotein which indicate a very close relationship of these lipids. As I pointed out in a previous publication (18) the properties of cholesterol as a lipid organizer result from a bulky, rigid body presenting many facets permitting strong van der Waals interactions with other lipid molecules. Evidence of this capacity is found for example, in the fact that unsaturated cholesterol esters, such as the cholesterol arachidonate recently synthesized by Mahadevan and Lundberg (38), are crystalline compounds.

Common Features of the Lipids of the Myelin Sheath

A general concept of complexes of cholesterol with the myelin sheath lipids, is best understood by the remarkable similarity in the structures of such lipids. This is shown in Figure 15, where typical examples

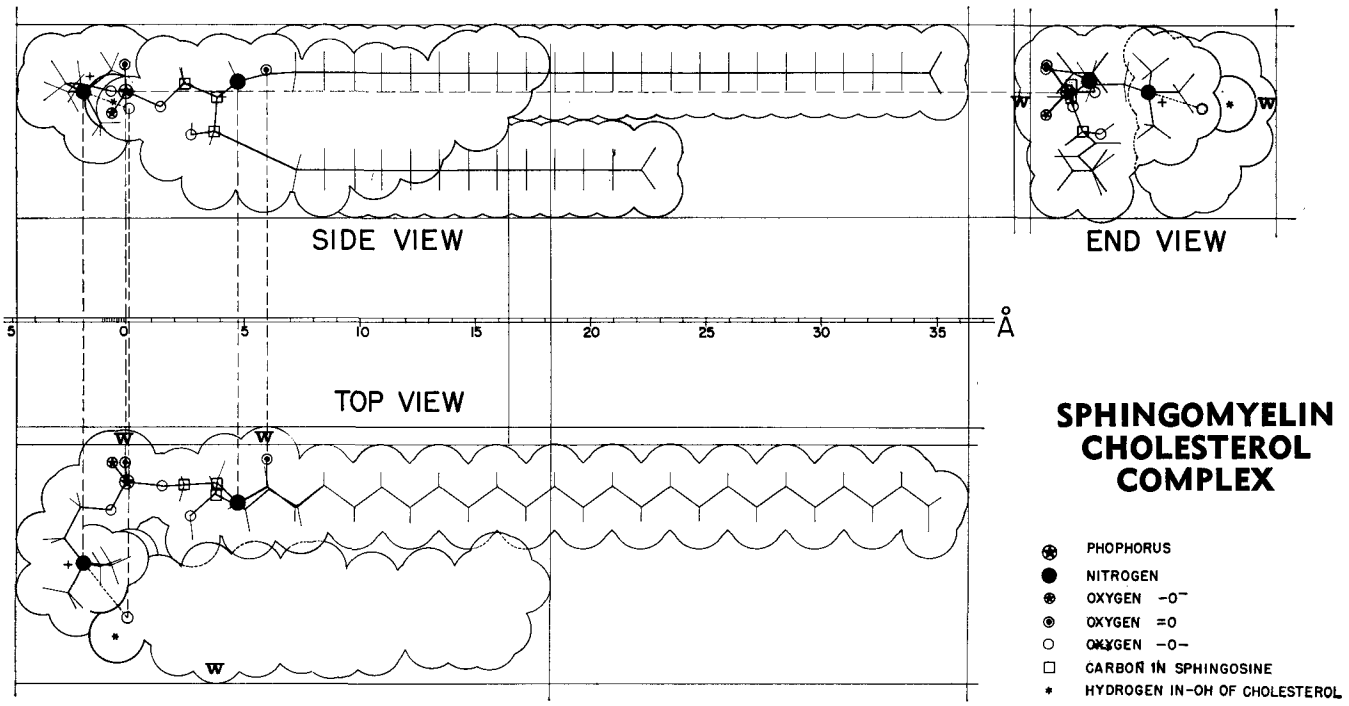

FIG. 17. Sphingomyelin-cholesterol complex. Note structural similarity with cholesterol-lecithin complex (Fig. 16), and bulges W.

of the two main classes formed by these lipids, i.e., the *phosphatidyl-* and *sphingolipids,* are represented.

It is immediately apparent that the sphingosine molecule is structurally equivalent to a monoglyceride having a fatty acid chain of 14 carbon atoms. The connection of the fatty acid to C_2 of the sphingosine molecule differs only from that found in the diglyceride moiety of the phosphatidyl lipid, as to the nature of the connecting atom. It can also be shown that the *cis* vinyl ether linkage of the *phosphatidal* lipids (plasmalogens) does not differ, either in the number of atoms involved or in overall effective dimensions from the corresponding group in phosphatidyl compounds.

As this Figure shows, the third chain of these lipids contains a common characteristic sequence indicated in heavy line. Starting from C_1 of glycerol or sphingosine, appear in zig-zag succession: an oxygen atom, an atom which is either phosphorus or carbon, an oxygen atom, two consecutive carbon atoms, and a polar group. These would seem the essential features required for this chain to qualify for admission in this lipid club. All other groups or substituents grafted onto this basic structure would only serve to confer distinctive properties. Computations of bond angles and distances of these basic elements also predict that a considerable similarity in overall distance and direction is to be expected. This observation might be of value for the synthesis of lipids acceptable to this system yet having desirable chemotherapeutic or pharmacological properties.

New Model of Cholesterol-phospholipid Complex

The complexes about to be described account for all established structural features of cholesterol (39, 40), the phosphatidyl and phosphatidal (41–46), and sphingolipids (47–58) of animal origin. The principle which led to the *cholesterol-lecithin complex* described in Figure 16 is that of maximum van der Waals interaction already discussed. For the lecithin molecule itself, this requires that fatty acid carbon chains lie in parallel zig-zag and close contact. The distance is then 4.17 Å, and even with only the 10-carbon pairs involved in the coupling of a straight chain and one with unsaturation beginning at C_9, the total interaction between chains is −13 Kcal., well above the −6 to −9 Kcal. required to form a stable complex. This configuration of the fatty acid chains corresponds to a strainless configuration of the whole molecule which is shown in this Figure. The phosphatidic chain, granted a coplanar configuration of its basic elements, assumes the position shown. The unsaturated section of the chain linked to carbon 2 of glycerol was also given a planar configuration, thus curving and ending up at points R, S or T depending on the number of double bonds. It must be pointed out that the resulting arrangement followed logically from the application of simple rules and without regard to cholesterol dimensions. However, it was found that when the cholesterol molecule was positioned for maximum attractive interaction with the phosphatide molecule (see above), it also fitted exactly between the choline end and the curved unsaturated chain of the latter molecule.

The situation at the cholesterol hydroxyl junction is as follows. The van der Waals perimeter of the oxygen atom of cholesterol, is tangent to the nitrogen and methyl groups of choline. Among the various interactions predictable for this cluster of 14 atoms where the N to O distance is 3.2 Å, are weak ion-dipole

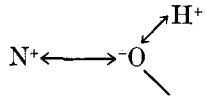

and hydrogen bond ($N\xrightarrow{+}:O$) (proton sharing) attractions. However, the van der Waals contribution alone is quite appreciable and should lend additional stability to the complex as a whole.

On the other hand, phosphatidyl lipids in nerve tissue contain a high proportion of unsaturated acids having the first double bond at C_9. Regardless of the number of double bonds which follow, the obstacle

TABLE III

Distribution of Lipids and Fatty Acids in Mammalian Nervous Tissue [a]

Lipid Type	Mole % Total Lipid (59)	Fatty Acids according to Chain Length [b] Weight % of lipid type S = saturated U = unsaturated												Source
		14		16		18		20		22		24 (+26)		
		S	U	S	U [c]	S	U [c]	S	U [c]	S	U [d]	S	U [e]	
Phosphatidyl.....	20	4.2		19.2	9.8	5.0	58.2		0.7		0.6			Human sciatic (60)
		96.4						1.3						
Sphingolipid.....	40	0.6		3.8		19.8	4.0	2.9	4.5	13.9	1.2	23.5	25.6	Beef spinal cord (61)
		50.7										49.1		
Cholesterol.....	40													

[a] Compilation of data from Johnson and Rossiter (59), Baker (60) and from Carroll (61).
[b] Odd number acids included in preceding even numbered series.
[c] First double bond at C_9 (Phosphatidyl) C_{18-1}: 8.3%; C_{18-1}: 49.7%; $C_{18-2} + C_{18-3}$: 8.6%.
[d] Double bond at C_{11}.
[e] Double bond at C_{15}.

preventing cholesterol from occupying a position further towards the end and alongside the phosphatide, is identically located.

The total van der Waals interaction between the two molecules is about −16 Kcal., including a minimum of −2 Kcal. for interaction at the top junction.

Substituting the choline group by the various other groups found in the phosphatidyl-phosphatidal series does not alter the geometry of the complex body or the coordinates of the phosphate ions. Furthermore, the substituted groups are all located within the confines of the body contours. With these groups, fewer atoms and distances about 0.5 Å shorter than in the case of choline, are involved at their junction with the cholesterol oxygen. Although the relative contributions of the various cohesional forces do vary in each case (ethanolamine, serine, inositol), the total interaction at this junction remains important. All lipids of the phosphatidyl-phosphatidal series present in myelin will fit therefore the model described for the cholesterol-lecithin complex.

A point of considerable interest in relation to the grouping of these elements in the myelin sheath, is that the effective length of a monounsaturated chain in this model is the same as that of a saturated chain shorter by two carbon atoms. Thus palmitic and oleic acid chains have the same effective length. Furthermore, the distance of the phosphorus atom to the tail end of these chains is 26 Å, i.e., half the phosphorus-to-phosphorus distance in the bimolecular lipid leaflet of myelin.

The Cholesterol-sphingomyelin Complex described in Figure 17 was evolved in a similar way. Justification for the existence of this complex through van der Waals interaction is even easier. Not only are there more carbon atoms involved in chain-to-chain interaction (14 instead of 10) but there are additional factors favouring interaction in the top section of the complex. Among these is a closer contact and the presence of the additional *erythro*-OH(C_3) group of sphingosine. The −OH group of cholesterol fits snugly against the choline group of sphingomyelin, and the cholesterol tail will just contact the bend in C_9 unsaturated acid chains representing about 10% of fatty acid chains in the sphingolipids.

The proposed models of bimolecular complexes of cholesterol with phosphati*dyl (dal)* and sphingolipids are thus basically similar. The cross sectional area is about 100 Å^2 in both cases. Only for phosphatidyl elements containing minor component fatty acids of myelin (diene, triene) should this area reach 113 Å^2. Cross sectional area measurements made by Dervichian from monolayers of cholesterol and egg lecithin have shown the following. For equimolecular proportions, the cross sectional area per molecule was 53 Å^2, corresponding to 106 Å^2 for the 1:1 cholesterol-lecithin complex.

For films containing a 3:1 molecular proportion of cholesterol and lecithin, the mean area per molecule was 42 Å^2. In this case also, the 44 Å^2 area predicted from the cholesterol-lecithin complex model and the cholesterol model (Fig. 7) is in excellent agreement with Dervichian's observation.

The Bimolecular Lipid Leaflet. For the following demonstration, a qualitatively correct, although only semiquantitatively exact distribution of lipids in the mammalian myelin sheath is sufficient. This was obtained (Table III) by compiling data from Johnson

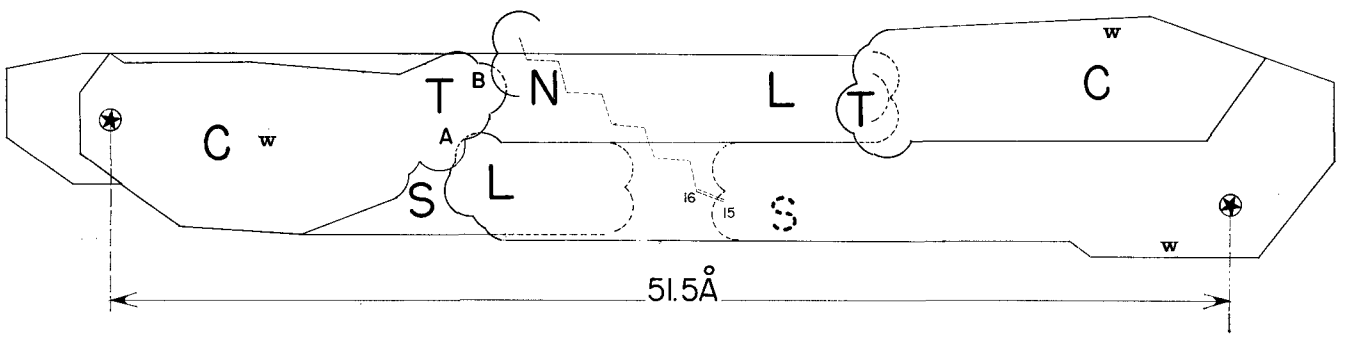

INTERDIGITATED CHOLESTEROL—SPHINGOMYELIN UNIT

FIG. 18. Interdigitated C–S complex of C_{24} sphingomyelin elements. C = cholesterol; S = sphingosine chain; L = lignoceric chain; T = cholesterol tail; N = position of tail end of nervonic acid chain when present. Contact occurs either at A for lignoceric chain or B for nervonic, a bump (H atom) fitting into dimple between adjacent H atoms on other molecule. Note bulges W on opposite sides and both ends of this unit. Cf. Figures 16 and 17.

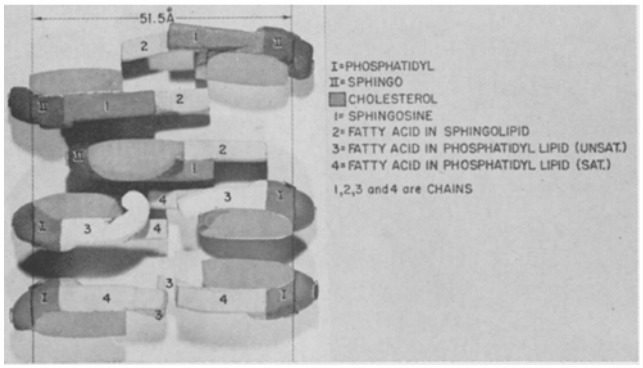

FIG. 19. Scale models of various cholesterol-lipid complexes. Only the critical dimensions are accurately represented. The black line on model head indicates position of phosphorus atom in phospholipids or of C atom I in the galactose of cerebrosides.

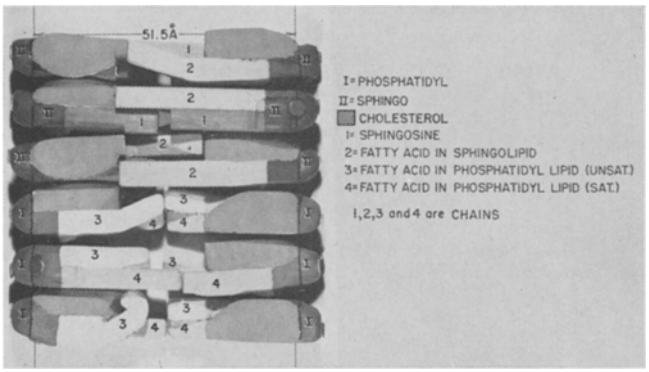

FIG. 20. Elements described on Figure 19 shown assembled. The sphingolipid complexes (II) are interdigitated, the sphingosine chains (1) being opposed, the fatty acid chains (2) of one complex unit butting against the cholesterol in the other one. The tail ends of the phosphatidyl complexes (I) are simply touching each other. The P–P distance (black lines) is 51.5 Å in all cases.

and Rossiter on cat, dog, rabbit, and human peripheral nerve (59), from Baker on the fatty acids in human sciatic nerve phosphatidyl lipids (60), and from Carroll (61) on beef spinal cord sphingolipid fatty acids. It is enough to know, for instance, that a very large proportion of the sphingolipid fatty acids is made up of C_{24} saturated and C_{24} unsaturated fatty acids. Also, that palmitic and oleic acid, which in our model have the same effective length, form the largest proportion of phosphatidyl lipid fatty acid, while small, approximately equal proportions of stearic and myristic acid are present in these acids.

As shown in Figure 18, the key to the arrangement of lipids to form a bimolecular leaflet of the observed width, appears to be the group formed by two cholesterol-sphingolipid complex units with either saturated or unsaturated chain of maximum length. When two such units are brought together tail-to-tail with the sphingosine chains in opposition, they interdigitate, resulting in an arrangement which involves considerable van der Waals interaction. As the diagram shows, the tail end of a C_{24} saturated chain fits under the tail of the opposed cholesterol while the tail end of the C_{24} monounsaturated chain butts against the tail end of cholesterol. The distance between phosphorus atoms in the resulting unit is 51.5 Å which is that observed by Finean for human myelin (33).

Figure 19 (top) shows the key units represented by idealized models where critical dimensions have been reproduced to scale. In these models, the black lines indicate the position of the phosphorus atoms in phospholipids or that of carbon atom 1 of galactose in the cerebrosides. From the typical phosphatidyl units shown below, it is evident that highly prevalent palmityl-oleyl units in direct opposition will produce the correct phosphorus-to-phosphorus distance with their tail ends in contact. Figure 20 shows various units assembled. The distribution of lipids (Table III) is such that one out of three bimolecular units could correspond to the key C_{24} model represented at the top. Note that the 4-Å gap noticeable between the two opposed sphingosine tails would allow the C_{20} sphingosine recently discovered by Majhofer and Prostenik (62) in horse and cow brain, to fit in. The second third of the bimolecular lipid units is mostly sphingolipid with shorter chains, some of which can be paired with C_{25} and C_{26} elements, thus forming units of standard length, while the remainder is made up of phosphatidyl elements. For about 75% of the latter, which contain at least one palmitic or oleic chain on each side, the phosphorus-to-phosphorus distance is automatically maintained. The pairing of C_{18} with C_{14} elements, which are present in about equimolecular amounts, would seem to solve the problem for another 10%. This leaves only elements shorter than C_{16}, i.e., linoleic, linolenic, and palmitoleic; and a very small proportion of highly unsaturated material of probable glial (mitochondrial) origin. Consequently, 60–66% of all bimolecular units would be long elements corresponding to the correct phosphorus-to-phosphorus distance.

For units involving shorter chains, this spacing could be maintained through anchorage to the common overlaying protein chains, by alignment of the cholesterol molecules resulting in maximum interunit interaction, and by the presence of water filling all intervening spaces. Under conditions of extreme dehydration, the shorter elements should be drawn towards the center of the bimolecular leaflet and the longer elements remain virtually undisturbed. Thus is explained the jagged electron micrographic appearance of the myelin layers in samples which have been fixed by certain techniques (32). Figure 21 shows an arrangement of various units seen from the protein side of the membrane. The role of slight

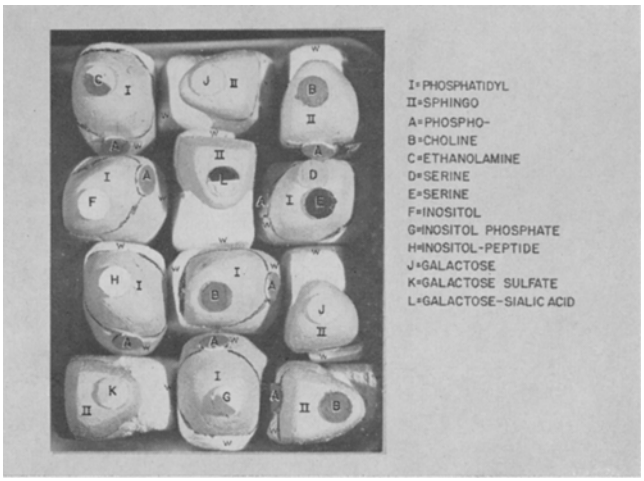

FIG. 21. Top view of assembled elements such as shown in Figures 19 and 20, describing the topography of the bimolecular lipid leaflet from the protein side. The protein in direct contact probably occurs as extended zig-zagging chains, some aminoacid limbs being planted in valleys, anchored by ionic linkages. The distribution shown is arbitrary. Note bulges W acting as spacers between elements. (Fig. 17).

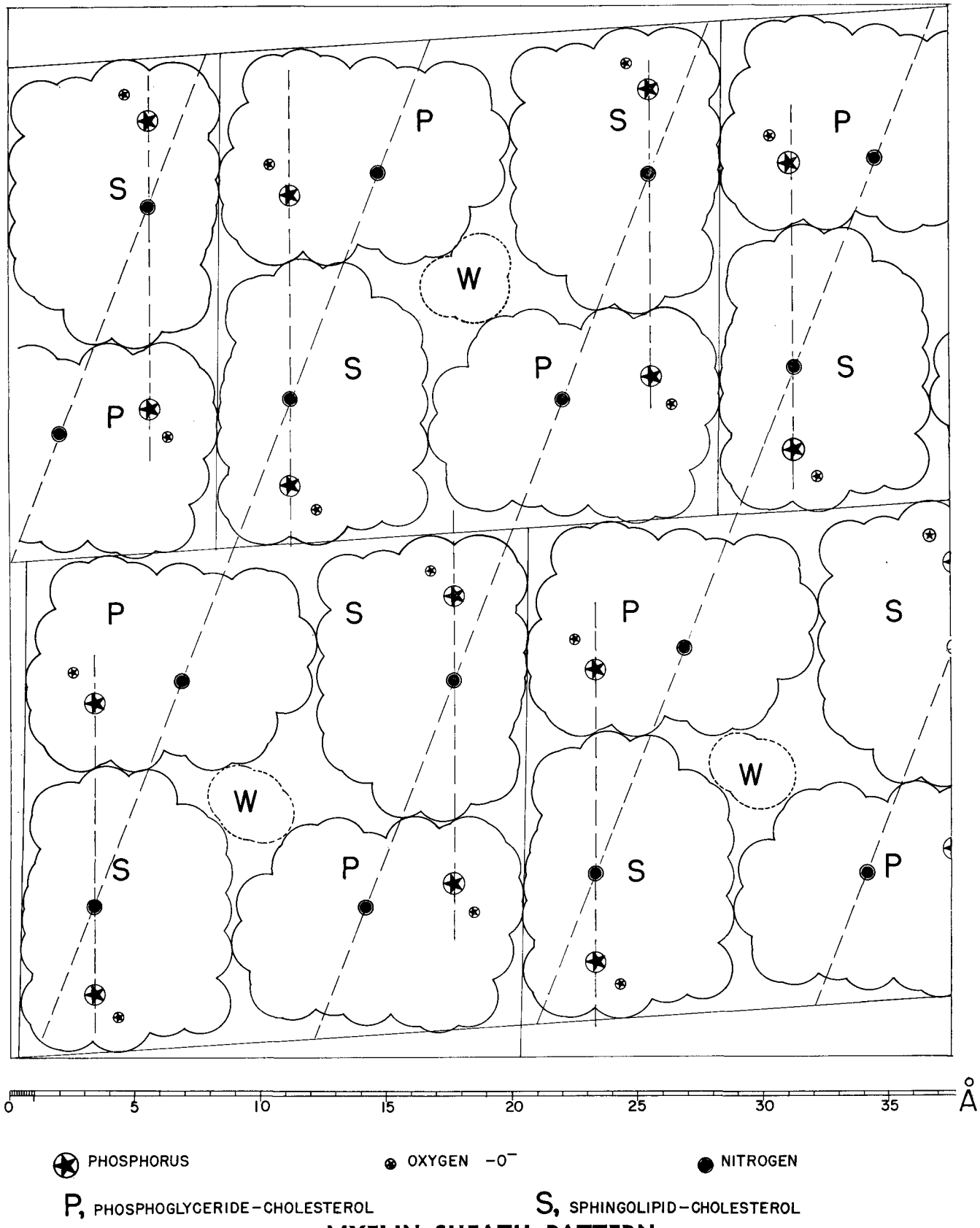

FIG. 22. Pattern obtained by grouping end views (Figs. 16,17) of lecithin-cholesterol (P) and sphingomyelin-cholesterol (S) elements. Alignment of nitrogens (choline) results when position of each unit is ⊥ to that of neighbour units. Considerable symmetry is then also obtained for position of other groups; also, excellent fit of unit contours. Water molecules in various positions shown as W.

bulges (W) appearing on two opposite sides of each complex unit (see also Fig. 18, W) could be to maintain some distance between adjacent units, thereby decreasing interunit interactions and the chance of complex dissociation. The spacing thus obtained also permits accommodation of chain hydroxyls, branched

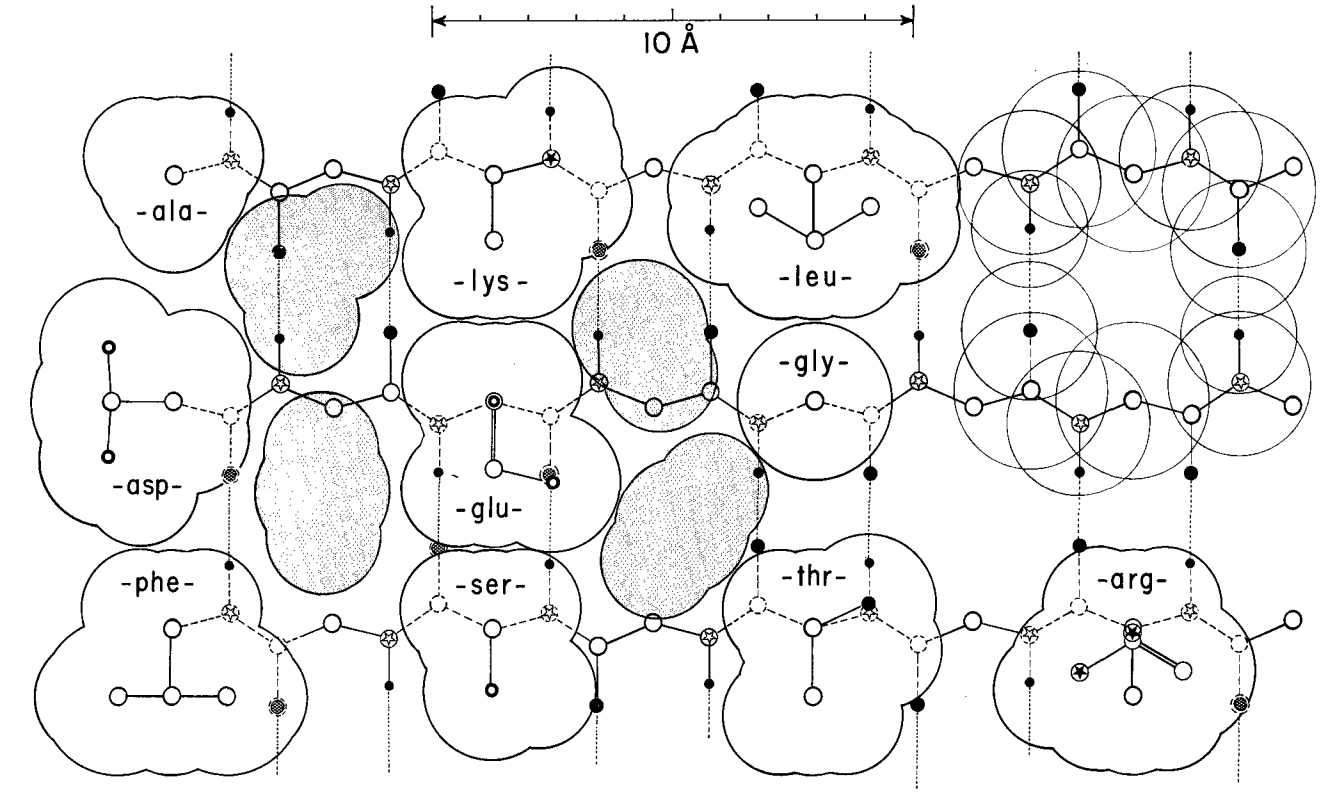

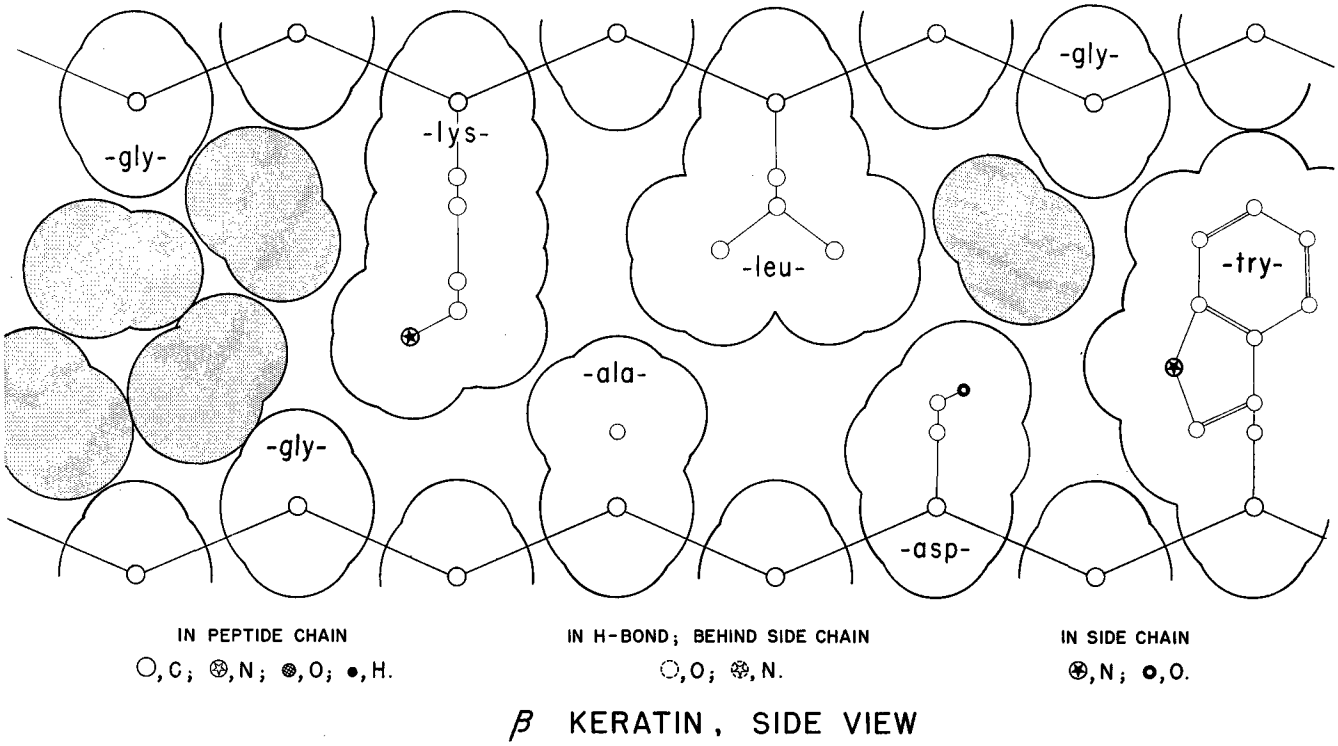

FIG. 23. (above) and 24. (below) van der Waals contours of amino acid side chains in two projections of β-keratin configuration (antiparallel). The amino acid sequence is different in each figure. Shaded areas represent water molecules between amino acid side chains. Symbols for center of atoms as indicated in the figure. From Vandenheuvel (18).

methyls, and tail ends of polyunsaturated chains.

Indeed, the complete acceptance of a considerable variety of known structural features by these models would appear to substantiate both their existence and the validity of the simple configurational principles used in their elaboration. This impression is further reinforced by the following considerations.

Figure 22 shows an end view of an arrangement of cholesterol lecithin (P) and cholesterol-sphingomyelin (S) complex units which is not representative

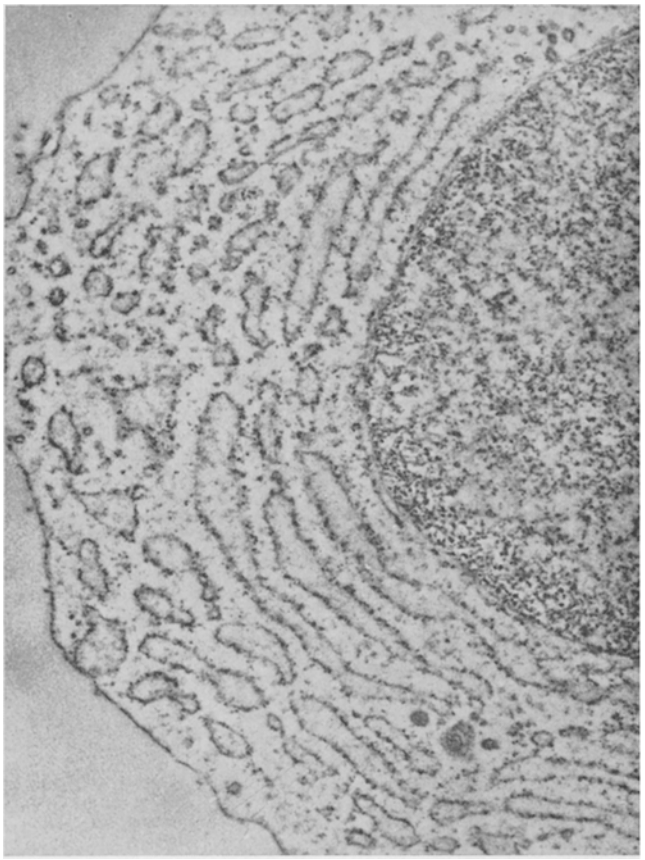

FIG. 25. Electron microscope view of plasma cell showing extensive cytoplasmic reticulum membranes. In many cells, this is the location of *protein synthesis* under control of RNA. The γ globulins involved in immune defence are synthesized in the plasma cell. From Howatson and Ham (67).

FIG. 26. Electron microscope image of mitochondrion showing typical membrane organization. In heterotrophic cells, mitochondria are responsible for basic respiratory *energy-transfer* process harnessing foodstuff oxidation energy (Krebs cycle) in the form of ATP-bound energy. From Howatson and Ham (67).

FIG. 27. High resolution electron micrograph of mitochondrion of spiral in tail of spermatozoid. Supplying energy for locomotion, thereby involved in *reproduction.* From André (68).

of the myelin sheath composition but will serve to illustrate a few points of particular interest. It should be noted that the projection of the P and S complexes and the location of ionic groups in these projections are not superimposable. The remarkable alignment of ionic groups which results from the simple arrangement described in the caption thus reveals unexpected basic elements of symmetry common to the two models. Second is the occurrence of pores which are of the size predicted by Solomon's estimation of pore radii in membranes (63). Such pores, which in this model communicate with the other side through the presumably water-filled spaces between monolayers could vary in diameter depending on the position of phosphatidyl elements. These, it must be remembered, are not interdigitated, in contradistinction to the sphingolipid elements, and are therefore capable of independent rotation around their main axis. Such movements need be only very slight either to block entirely the passage of molecules of water (w) or to permit a considerable increase of water diffusion. A one-Å increase in diameter would even allow the passage of a molecule the size of glycerol. The required adjustments of the phosphatidyl unit could easily be commanded by temporary reshuffling of ionic and hydrogen bonds determining the position of a P complex. Such modification could be brought about by local impact of the diffusing molecule (or ion) with the protein limb anchoring the P element or with the P element itself. Third, there is no indication from this type of pore geometry, of a selective restraint to the continuous diffusion in either direction of small cations having approximately the same diameter. This conclusion fits the results of

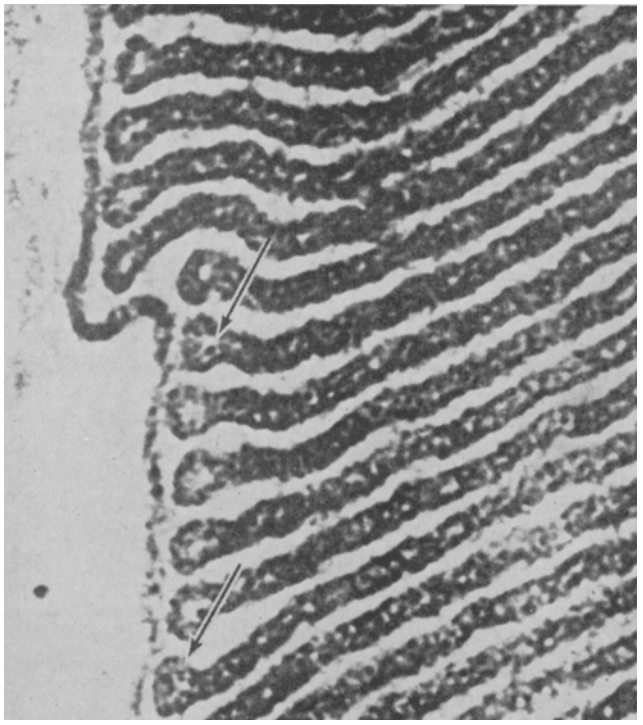

FIG. 28. Electron micrograph of retinal-rod outer segment where membrane system involving photopigment complexes (Rhodopsin), constitute basic photoreceptor apparatus involved in *vision*. From Fernández-Morán (1).

recent and precise experiments by Tasaki (64) on the giant squid axon membrane, indicating no significant difference in either influx or efflux for either Na^+ or K^+ ions. These are but a few of the many speculations that could be made with a diagram truly representative of the membrane topography.

Mapping of the myelin membrane in the manner illustrated here will require the use of short X-ray reflections corresponding to the spacing of phosphorus atoms in a direction perpendicular to the long axes of the units, i.e., vertical for this diagram. Representative, detailed analyses of the lipids in the same tissue will be needed to bring such work to completion. This will require, not only the refined analytical methods described by Rouser in another paper in this symposium, but also a careful assessment of the lipid contribution by extraneous tissue, and control of lipid losses occurring in the course of sample preparation. Such losses were demonstrated by Lovelock (65) and encountered by Marinetti et al. (66) in the processing of other tissues.

The smallest amount of information on the nature of the overlaying protein (Fig. 23,24), such as fragmental data on its aminoacid sequence, would be extremely helpful in this research.

The myelin sheath of nerve is but one of the multitude of cases involving membranes in cells of animal and vegetable filiation. Figures 25, 26 (67), 27 (68), and 28 (1) constitute a very succinct testimony of the ubiquity of membranes and of their involvement in the most diverse and important functions. On the other hand, there is abundant evidence indicating the important role played by these membranes in the related functions (69). A detailed model of the *unit membrane* (70) would undoubtedly be of practical value in many fields of biology and medicine.

ACKNOWLEDGMENTS

Contribution No. 144, Animal Research Institute, Research Branch, Canada Dept. of Agriculture, Ottawa, Ontario.

REFERENCES

1. Fernández-Morán, H., Circulation, *26*, 1039 (1962).
2. Morris, I. H., and J. Husband, "Practical Plane and Solid Geometry," Longmans, Green & Co., New York, 1903.
3. Jackson, H. R., and F. A. Vandenheuvel, J. Photog. Sci., in press.
4. Waugh, D. F., "Macromolecular Complexes," Ed. M. V. Edds, Jr., The Ronald Press Co., New York, 1961, p. 7.
5. Setlow, R. B., and E. C. Pollard, "Molecular Biophysics," Addison-Wesley Publishing Co. Inc., Reading, Mass., 1962, p. 157.
6. Fisher-Hjalmars, I., Advance Course, Winter Institute in Quantum Chemistry and Solid State Physics, Sanibel Island, Florida, U.S.A., (1962).
7. Pauling, L., "The Nature of the Chemical Bond," 3rd ed., Cornell University Press, 1960, p. 260.
8. Bartell, L. S., Tetrahedron, *17*, 177 (1962).
9. Wilson, E. B., Jr., "Advances in Chemical Physics," Vol. II, Interscience Publishers, Inc., New York, 1959, p. 367.
10. Bunn, C. W., and D. R. Holmes, Discuss. Faraday Soc., *25*, 95 (1958).
11. Salem, L., Can. J. Biochem. Physiol., *40*, 1287 (1962).
12. Pauling, L., "The Nature of the Chemical Bond," 3rd ed., Cornell University Press, 1960, chap. 12.
13. Bernal, J. D., "Hydrogen Bonding," Symposium, IUPAC, Ljubljana, Yugoslavia, 1957, Pergamon Press, New York, 1959, p. 7.
14. Coulson, C. A., *Ibid.*, p. 339.
15. Lippincott, E. R., J. N. Finch, and R. Schroeder, *Ibid.*, p. 361.
16. Gurd, F. R. N., and P. E. Wilcox, Advanc. Protein Chem., *11*, 311 (1956).
17. Rakhit, S., and Ch. R. Engel, Can. J. Chem., *40*, 2163, (1962).
18. Vandenheuvel, F. A., Can. J. Biochem. Physiol., *40*, 1299, (1962).
19. Eckwall, P., R. Ekholm, and A. Norman, Acta Chem. Scand., *11*, 693 (1957).
20. Pauling, L., "The Nature of the Chemical Bond," 3rd ed., Cornell University Press, 1960, p. 138.
21. Schachtschneider, J. H., and R. J. Snyder, Spectrochimica Acta, *19*, 117 (1963).
22. Lide, D. R., Jr., Tetrahedron, *17*, 125 (1962).
23. Stoicheff, B. P., *Ibid.*, *17*, 135 (1962).
24. Bastiansen, D., and M. Tratteberg, *Ibid.*, *17*, 147 (1962).
25. Pauling, L., "The Nature of the Chemical Bond," 3rd ed., Cornell University Press, 1960, p. 230.
26. Geren, B. B., Exp. Cell Res., *7*, 558 (1954).
27. Maturna, H. R., J. Biophys. Biochem. Cytol., *7*, 107 (1960).
28. Peters, A., *Ibid.*, *7*, 121 (1960).
29. Smidt, W. J., Z. Zellforsh., *23*, 657 (1936).
30. Schmitt, F. O., R. S. Bear, and K. J. Palmer, J. Cellular Comp. Physiol., *18*, 3 (1941).
31. Danielli, J. F., and H. Davson, "The Permeability of Natural Membranes," Cambridge University Press, 1943.
32. Finean, J. B., J. Biophys. Biochem. Cytol., *8*, 13 (1960).
33. Finean, J. B., Circulation, *26*, 1151 (1962).
34. Finean, J. B., Experiencia, *9*, 17 (1953).
35. Willmer, E. N., Biol. Rev., *36*, 368 (1961).
36. Dervichian, D. G., "Surface Phenomena in Chemistry and Biology," Pergamon Press, New York, 1958, p. 70.
37. Kramer, K., Acta Medica Scand., *170*, supp. 372 (1961); *Ibid.*, *171*, 413 (1962).
38. Mahadevan, V., and W. O. Lundberg, J. Lipid Res., *3*, 106 (1962).
39. Fieser, L. F., and M. Fieser, "Steroids," Reinhold Publishing Corp., New York, 1959.
40. Kritchevsky, D., "Cholesterol," John Wiley and Sons Inc., New York, 1958.
41. Garvin, J. E., and M. L. Karnowsky, J. Biol. Chem., *221*, 211 (1956).
42. Baer, E., Canad. J. Biochem. Physiol., *34*, 288 (1956).
43. Tattrie, N. H., J. Lipid Res., *1*, 60 (1959).
44. Hannahan, D. J., H. Brockerhoff, and E. J. Barron, J. Biol. Chem., *235*, 1917 (1960).
45. Norton, W. T., E. L. Gottfried, and M. M. Rapport, J. Lipid Res., *3*, 456 (1962).
46. Hawthorne, J. N., *Ibid.*, *1*, 255 (1960).
47. Kiss, J., G. Fodor, and D. Banfi, Helv. Chim. Acta, *37*, 1471, (1954).
48. Marinetti, G., and E. Stotz, J. Am. Chem. Soc., *76*, 1345 (1954.
49. Mislow, K., *Ibid.*, *74*, 5155 (1952).
50. Carter, H. E., and Y. Fujimo, J. Biol. Chem., *221*, 879 (1956).
51. Carter, H. E., and W. P. Norris, *Ibid.*, *145*, 709 (1942).
52. Carter, H. E., D. Shapiro, and J. B. Harrison, J. Am. Chem. Soc., *75*, 1007 (1953).
53. Klenk, E., and co-workers, Z. Physiol. Chem., *153*, 74 (1926); *157*, 291 (1926); *185*, 169 (1929); *235*, 24 (1935); *268*, 50 (1941); *273*, 76 (1942); *288*, 216 (1951); *299*, 48 (1955).
54. Rouser, G., J. F. Berry, G. Marinetti, and E. Stotz, J. Am. Chem. Soc., *75*, 310 (1953).
55. LeBaron, F. N., and J. Folch, Physiol. Rev., *37*, 539 (1957).
56. Radin, N. S., and Y. Akahori, J. Lipid Res., *2*, 335 (1961).
57. Carter, H. E., J. A. Rothfus, and R. Bigg, *Ibid.*, *2*, 228 (1961).
58. Goldberg, I. H., *Ibid.*, *2*, 103 (1961).
59. Johnson, A. C., and R. J. Rossiter, Biochem. J., *43*, 578 (1948).
60. Baker, R. W. R., *Ibid.*, *79*, 642 (1961).
61. Carroll, K. K., J. Lipid Res., *3*, 263 (1962).
62. Majhofer Oreščanin B., and M. Prostenik, Croat. Chem. Acta, *33*, 239 (1961).
63. Solomon, A. K., "Membrane Transport and Metabolism," Symposium, Prague, Czechoslovakia, 1960, Academic Press, New York, 1961, p. 94.
64. Tasaki, I., J. Gen. Physiol., *46*, 766 (1963).
65. Lovelock, J. E., Biochem. J., *60*, 629 (1955).
66. Marinetti, G. V., J. Erbland, and E. Stotz, J. Biol. Chem., *233*, 562 (1958).
67. Howatson, A. F., and A. W. Ham, Can. J. Biochem. Physiol., *35*, 549 (1957).
68. André, J., J. Ultrastructure Res., supp. 3, Academic Press, New York, 1962, p. 89.
69. Quastel, J. H., "Membrane Transport and Metabolism," Symposium, Prague, 1960, Ed. A. Kleinzeller and A. Kotik, Academic Press, New York, 1960, p. 512.
70. Robertson, J. D., Biochem. Soc. Symposia, Cambridge, England, *16*, 3 (1959).

[Received April 23, 1963—Accepted July 27, 1963]